University of Alberta

Characterization of *Cecr2* expression and the *Cecr2*$^{Gt(45Bic}$ mutation on different mouse genetic backgrounds

By

Tanya May Ames

©

A thesis submitted to the Faculty of Graduate Studies and Research in partial fulfillment of the requirements for the degree of Master of Science

In

Molecular Biology and Genetics

Department of Biological Sciences

Edmonton, Alberta

Fall 2006

Library and Archives Canada

Published Heritage Branch

395 Wellington Street
Ottawa ON K1A 0N4
Canada

Bibliothèque et Archives Canada

Direction du Patrimoine de l'édition

395, rue Wellington
Ottawa ON K1A 0N4
Canada

Your file Votre référence
ISBN: 978-0-494-22220-1
Our file Notre référence
ISBN: 978-0-494-22220-1

NOTICE:
The author has granted a non-exclusive license allowing Library and Archives Canada to reproduce, publish, archive, preserve, conserve, communicate to the public by telecommunication or on the Internet, loan, distribute and sell theses worldwide, for commercial or non-commercial purposes, in microform, paper, electronic and/or any other formats.

The author retains copyright ownership and moral rights in this thesis. Neither the thesis nor substantial extracts from it may be printed or otherwise reproduced without the author's permission.

AVIS:
L'auteur a accordé une licence non exclusive permettant à la Bibliothèque et Archives Canada de reproduire, publier, archiver, sauvegarder, conserver, transmettre au public par télécommunication ou par l'Internet, prêter, distribuer et vendre des thèses partout dans le monde, à des fins commerciales ou autres, sur support microforme, papier, électronique et/ou autres formats.

L'auteur conserve la propriété du droit d'auteur et des droits moraux qui protège cette thèse. Ni la thèse ni des extraits substantiels de celle-ci ne doivent être imprimés ou autrement reproduits sans son autorisation.

In compliance with the Canadian Privacy Act some supporting forms may have been removed from this thesis.

While these forms may be included in the document page count, their removal does not represent any loss of content from the thesis.

Conformément à la loi canadienne sur la protection de la vie privée, quelques formulaires secondaires ont été enlevés de cette thèse.

Bien que ces formulaires aient inclus dans la pagination, il n'y aura aucun contenu manquant.

Canada

Abstract

Neural tube defects (NTDs), the second most common birth defect in humans, have complex genetic and environmental causes. One gene involved in NTDs is *Cecr2* and a percentage of *Cecr2* homozygous mutant mice develop the NTD exencephaly. CECR2 forms a chromatin remodeling complex called CERF, therefore it is likely that CECR2 has a role in transcriptional regulation of other genes.

In the current study the following were investigated. The *Cecr2* mutation was analyzed on different mouse genetic backgrounds and the penetrance of the exencephaly phenotype differs depending on the background. Female mutant embryos develop exencephaly more frequently than males. Two splice variants of *Cecr2* are expressed and an anti-Cecr2 antibody was developed for use in further characterization of the mutation and normal Cecr2 function. Further investigation into which aspect of cranial neural tube closure is disrupted in the *Cecr2* mutant mice will help elucidate the role Cecr2 has in neurulation.

Acknowledgements

I would like to thank everyone that has assisted me in the production of this thesis. In particular I would like to extend my gratitude to all those individuals who have helped with the maintenance of the mouse colony including organizing, ear notching, genotyping, dissecting and general support when the mice seem like too much to handle. These people include Melanie Kardel, Courtney Davidson, Angela Keuling, Amanda Campbell, Twila Yobb, Adam Tassone and Jennifer Pockrant. Without all of these people this study would not have been possible.

I would also like to thank the person who began this project, Graham Banting. He was always willing to discuss the project with me and give his insight into what things to try next.

I would like to thank Jack Scott in the microscopy unit as without his expertise the figures in this study, in particular the embryo photographs, would not have been possible. Jack also helped me produce several posters and was always ready to help in any way.

I would like to thank the McDermid lab especially Twila Yobb, Stephanie Maier and Melanie Kardel for teaching me so many techniques. The entire McDermid lab is thanked for their constant support and for always offering to help with washes during a class, troubleshooting something that is not working or just offering supportive words.

I would like to extend an extra thanks to Amanda Campbell for all of her help on the editing of my thesis, while planning her wedding and studying to become an air traffic controller. I owe a great deal of thanks to my family and friends in Ottawa, Fredericton, Ft. Myers, Vancouver, Vermont and here in Edmonton. Without each and every one of them I would not have completed this degree.

Table of Contents

Chapter 1. Introduction **1**

1.1. Neural tube closure and defects 1
1.1.1. Neurulation 1
1.1.2. Neural tube defects 2
1.1.4. Cranial and caudal neural tube closure 6

1.2. Chromatin remodeling 8
1.2.1. Chromatin remodelling: an overview 8
1.2.2. The ISWI and SWI/SNF families 10
1.2.3. SNF2L containing complexes 11

1.3. CECR2/Cecr2 13
1.3.1. Chromosomal location 13
1.3.2. CECR2/Cecr2 potential function 14

1.4. Phenotype associated with *Cecr2* mutation 15

1.5. Research objectives 16

Chapter 2. Materials and Methods **20**

2.1. Mouse colony upkeep 20
2.1.1. Mouse housing 20
2.1.2. Mouse breeding 20
2.1.3. Euthanasia 21

2.2. Embryo manipulation 21
2.2.1. Embryo dissection 21
2.2.2. X-gal staining 21

2.3. Nucleic acid isolation 22
2.3.1. Mouse genomic DNA isolation 22
2.3.2. DNA extraction from agarose gels 23
2.3.3. RNA isolation 23

2.4. PCR 24
2.4.1. RT-PCR 24
2.4.2. Sequencing reactions 24
2.4.3. PCR reactions 25
2.4.4. *Cecr2*^{Gt45Bic} mutation genotyping PCR 26

2.5. Characterizing the *Cecr2*^{Gt45Bic} mutation on BALB/c, FVB/N and 129P2/ola genetic backgrounds 27
2.5.1. Congenic line production 27
2.5.2. Penetrance data collection 28

2.6. Anti-Cecr2 antibodies 29
2.6.1. Anti-Cecr2 pep A, B, C and D production 29
2.6.2. Protein extraction 30
2.6.3. Western blot using nitrocellulose membrane 30

2.6.4. Affinity purification 32
2.6.5. Western blot using PVDF membrane 33
2.6.6. Competition assay 34

Chapter 3. Results 39

3.1. The penetrance of exencephaly differs depending on mouse genetic background 39

3.2. Female mutant embryos develop exencephaly more frequently 40

3.3. *Cecr2*^{Gt45Bic} reporter gene expression on the incipient congenic BALB/c genetic background 41

3.4. *Cecr2*^{Gt45Bic} reporter gene expression just after neural tube closure on the BALB/129P2 genetic background 42

3.5. *Cecr2* alternative splicing 43

3.6. Creation of anti-Cecr2 antibodies 44

3.7. Analysis of anti-Cecr2 peptide A, B, C and D antibodies 44

3.8. Analysis of anti-peptide WB antibodies 46

Chapter 4. Discussion 64

4.1. Mouse genetic background affects the penetrance of the NTD exencephaly in mice homozygous for the *Cecr2*^{Gt45Bic} mutation. 64

4.2. The FVB/N mouse genetic background has one or more modifier genes that affect neural tube closure and/or Cecr2 function. 66

4.3. Female embryos that are homozygous for the *Cecr2*^{Gt45Bic} mutation develop exencephaly at a higher frequency than males. 69

4.4. *Cecr2* expression is widespread at the time of neural tube closure but shows more localized expression at later developmental stages. 71

4.5. Three anti-Cecr2 antibodies were created and used to confirm that Cecr2 protein is expressed past the genetrap in homozygous mutant *Cecr2*^{Gt45Bic} mice. 73

4.6. There are 2 main splice variants of *Cecr2*. 73

4.7. Is CERF involved in neurulation? 75

4.8. Future directions 78

4.8.1. Confirm the CERF complex forms in mice and determine if Cecr2 is involved in any other complexes. 78

4.8.2. Characterization of the *Cecr2* mouse mutants to determine the role Cecr2 plays during neurulation. 80

4.8.3. Investigate the BALB/c and FVB/N genetic backgrounds to determine what neurulation specific modifier genes differ between the strains, what part of neurulation is affected by these genes and if there is a sex linked difference in neurulation. 83

4.8.4. The role of Cecr2 in other developmental pathways. 83

4.9. Significance of this work 83

Chapter 5. Bibliography 86

List of Tables

Table 1. Primer sequences used in this study.....36

Table 2. Location of Cecr2 peptides used in the production of anti-Cecr2 antibodies.....38

Table 3. The penetrance of exencephaly in *Cecr2*$^{Gt45Bic/Gt45Bic}$ mice is variable depending on mouse genetic background.....48

Table 4. Female embryos homozygous for the *Cecr2*^{Gt45Bic} mutation have a higher penetrance of exencephaly than males with the same homozygous mutation on two different genetic backgrounds.....51

Table 5. Male/female ratio of *Cecr2*^{Gt45Bic} mutant embryos with exencephaly.....52

Table 6. Potential PCR products that can be produced from *Cecr2* cDNA using PCR primer sets CECR2 F21/CECR2 R11 or CECR2 F21/Cecr2 10eR1.....55

List of Figures

Figure 1. Schematic diagram of the four neural tube closure points and the associated NTD phenotype 18

Figure 2. Schematic diagram of the mouse *Cecr2* gene 19

Figure 3. Location of the genetrap within *Cecr2* intron 7 and a sample genotyping PCR gel electrophoresis picture 37

Figure 4. Mating scheme to transfer the $Cecr2^{Gt45Bic}$ mutation from a mixed genetic background onto BALB/c, FVB/N and 129P2/ola genetic backgrounds 49

Figure 5. X-gal staining showing expression of the Cecr2-LacZ fusion protein in the congenic BALB/c genetic background 50

Figure 6. X-gal staining of 9.5 dpc mouse embryos showing expression of the Cecr2-LacZ fusion protein after neural tube closure 53

Figure 7. Potential alternatively spliced transcripts produced from the *Cecr2* gene 54

Figure 8. Expression analysis of *Cecr2* in 12.5 dpc embryo using RT-PCR 56

Figure 9. Expression analysis of *Cecr2* in adult mouse brain, liver and 12.5 dpc embryo using RT-PCR 57

Figure 10. Location of the anti-Cecr2 epitopes 58

Figure 11. Western blot analysis to determine the specificity of the anti-Cecr2 pepC antibody in mouse tissues 59

Figure 12. Transcriptional read-through occurs past the $Cecr2^{Gt45Bic}$ genetrap mutation and the anti-Cecr2 pepC antibody detects the resulting protein in heterozygous and homozygous mutant mice 60

Figure 13. A competition assay to determine the specificity of the anti-Cecr2 pepA antibody using Western blot analysis 61

Figure 14. A competition assay to determine the specificity of the anti-Cecr2 pepC antibody using Western blot analysis 62

Figure 15. Preliminary testing of the anti-Cecr2 pepWB antibody using Western blot analysis 63

List of Abbreviations

aa	Amino acid
ACF	ATP-utilizing, chromatin assembly and remodeling complex
APS	Ammonium persulfate
AT hook	Adenine/thymine hook
ATP	Adenosine triphosphate
ATRX	α-thalassemia/mental retardation syndrome X-linked
Axd	*Axial defects*
ß-geo	Genetrap cassette including *LacZ* coding region and neomycin resistance selectable marker
BAZ1	Bromodomain adjacent to zinc finger 1 motif
BMP	Bone morphogenetic protein
bp	Base pair
BPTF	Bromodomain PHD finger transcription factor
BRG1	*Brahma like gene one*
BRM	*Brahma*
BSA	Bovine serum albumin
BSLAS	Biological Sciences laboratory animal services
cDNA	complementary DNA
CERF/CeRF	CECR2-containing remodeling factor (human and mouse respectively)
CECR2/Cecr2	Cat eye syndrome chromosome region, candidate 2 (human and mouse respectively)
CES	Cat eye syndrome
CHD/Mi-2	Chromodomain helicase DNA binding
CHRAC	Chromatin accessibility complex
cM	Centimorgan
CP	Carrier protein
Crc	*Circletail*
CSB	Cockayne syndrome protein B
Ct	*Curly tail*
Da	Daltons
DDT	DNA binding homeobox and different transcription factors
DEPC	Diethyl pyrocarbonate
DLHPs	Dorsolateral hinge points
DNA	Deoxyribonucleic acid
dNTPs	Deoxynucleotide triphosphates
Dpc	*Days post coitus*
DTT	Dithiothreitol
EDTA	Ethylene diamine tetraaacetic acid
Efna5	*Ephrin-A5*
Epha7	*Eph-A7*
ES	Embryonic stem
ESTs	Expressed sequence tags
EtBr	Ethidium bromide

EtOH	Ethanol
H. sa.	*Homo sapiens*
HSLAS	Health sciences laboratory animal services
ISWI	Imitation switch (x at beginning signifies *Xenopus*)
KLH	Keyhole limpet hemocyanin
LacZ	ß-galactosidase
Lp	*Loop-tail*
m	$Cecr2^{Gt45Bic}$
MBSU	Molecularbiology service unit
MeOH	Methanol
MHP	Median hinge point
M. mu.	*Mus Musculus*
NaOAc	Sodium acetate
NLS	Nuclear localization signal
NoRC	Nucleosome-remodelling complex
nt	Nucleotide
NTDs	Neural tube defects
NURF	Nucleosome-remodeling factor (h at beginning signifies human)
Opb	*Open brain*
+	Wild type
PAGE	Polyacrylamide gel electrophoresis
Pax 6	*Paired box gene 6*
PBS	Phosphate buffered saline
PCR	Polymerase chain reaction
PVDF	Polyvinylidene fluoride
RbAp48/46	Retinoblastoma-associated protein 48/46
RNA	Ribonucleic acid
rpm	Revolutions per minute
RSF	Remodelling and spacing factor
RT-PCR	Reverse transcription PCR
SDS	Sodium dodecyl sulfate
Shh	*Sonic hedgehog*
Shrm	*Shroom*
SNF2H/Snf2h	SWI/SNF related, matrix associated, actin dependant regulator of chromatin, subfamily a, member 5 (human and mouse respectively)
SNF2L/Snf2l	SWI/SNF related, matrix associated, actin dependant regulator of chromatin, subfamily a, member 2 (human and mouse respectively)
Sox9	*Sex determining region-box 9*
Sp	*Splotch*
SWI/SNF	Mating type switching/sucrose non-fermenting
WCRF	WSTF-related chromatin-remodelling factor
WICH	WSTF-ISWI chromatin-remodeling complex
Wnt	Wingless-type MMTV integration site family
Xn	*Exencephaly*

Chapter 1. Introduction

1.1. Neural tube closure and defects

1.1.1. Neurulation

Neural tube closure occurs very early in embryonic development. The neural tube is closed by day 28 in humans and between days 8-10 in mice (Harris and Juriloff 1999; Sadler 2005). Neurulation, the process of forming the neural tube, is initiated by sonic hedgehog (Shh) signals from the notochord. These signals induce the overlying ectoderm to become neuroectoderm by suppressing the bone morphogenetic protein (BMP) and wingless-type MMTV integration site family (Wnt) signals necessary for epidermal cell fate (Sadler 2005). The cells destined to form the neural tube elongate and form a region of cuboidal cells called the neural plate. Shh signalling from the notochord also induces the ventralization of the neural plate by creating a region called the floor plate. The floor plate also expresses *Shh*, an important regulator of neurulation. The neural plate then becomes divided into two folds by the formation of the median hinge point (MHP) at the midline. The two neural folds elevate towards one another and the tips eventually fuse at specific regions along the midline. Fusion then continues from these initial sites until a tube is created (Sadler 2005).

The specific regions along the midline where fusion is initiated have been well studied in mice (Juriloff et al. 1989). The neural tube begins closure by fusion of the two neural folds at the hindbrain/cervical boundary. The two folds fuse together at this point, known as closure point 1, at the 2-8 somite stage in mice depending on the genetic background **(Figure 1 A)**. Fusion then proceeds in a bidirectional manner from closure 1. The second initiation site, closure 2, usually occurs at the forebrain/midbrain boundary at the

9-14 somite stage and again fusion continues in a bidirectional manner **(Figure 1 A)**. The location of the second fusion point has been shown to occur in variable regions of the forebrain and midbrain depending on the mouse genetic background (Juriloff et al. 1989). The third initiation site occurs at the most rostral end of the forebrain and proceeds caudally. This third closure point closes the anterior neuropore at the 12-17 somite stage **(Figure 1 A)** (Macdonald et al. 1989; Copp et al. 2003). Some sources also report a closure 4 site. Closure 4 does not occur by fusion of the neural folds, but by the elongation of a membrane rostrally from the caudal end of the hindbrain. The membrane will cover the hindbrain (Golden and Chernoff 1993). As closure 4 is not a fusion point some sources only report the first three closure points described above (Copp 2005).

In humans, closure 1 and 3 are present, however closure 2 has been inconsistently observed (Copp et al. 2003). Some argue that human embryos have a relatively smaller midbrain than mouse embryos, just after neural tube closure. Therefore the closure 2 site is unnecessary in humans and is thus absent (Copp 2005). However, fusion at closure 2 may simply be initiated at more variable regions in humans as is seen in mice. It may also be that closure 2 is located very close to closure 3 and is not detected. Perhaps, due to the small numbers of human embryos studied at the correct time point, the potential closure 2 site is not always detected.

1.1.2. Neural tube defects

Failure of any of the different neural tube closure points to close causes neural tube defects (NTDs). NTDs are a common birth defect in humans second only to heart defects. NTDs occur at a frequency of approximately 1 in 1000 births (Copp et al. 2003). NTDs occur when the neural folds fail to elevate, bend, or fuse at different locations

along the developing neural tube. This failure may result in such defects as anencephaly (exencephaly in mice) in the cranial region and/or spina bifida in the spinal region **(Figure 1 B and C)**. Failure of the neural tube to close in early gestation can also cause other defects including craniorachischisis where the entire midbrain and spinal region remain open, spina bifida occulta where there is a skin covering over the open neural tube, and split face. However, the two most common NTDs in both humans and mice are spina bifida and anencephaly (Harris and Juriloff 1999).

Although usually at the forebrain/midbrain boundary, closure 2 location in mice has been described in a variety of different genetic backgrounds and occurs at variable regions (Macdonald et al. 1989; Golden and Chernoff 1993; Copp et al. 2003). Closure 2 can form rostrally in the forebrain region or caudally in the midbrain region. It has been suggested that the more rostral the location of closure 2, the more susceptible the mouse strain may be to developing exencephaly (Berube et al. 2002; Copp et al. 2003). In some mouse genetic backgrounds such as SELH/Bc, which are susceptible to developing exencephaly, closure 2 does not form at all (Macdonald et al. 1989). This is also the case in the *open brain* (*opb)* mutant mouse model (Gunther et al. 1994).

Mutant mouse lines lacking closure at site 1 (*Circletail* [*Crc*], *Loop-tail* [*Lp*], *crash* and *dishevelled 1/2* double knockout) develop craniorachischisis but not other NTDs (Kibar et al. 2001; Copp et al. 2003; Murdoch et al. 2003). These mutant lines all have defects in the planar cell polarity pathway, which is important for convergent extension of the mouse embryo. Convergent extension (movement of cells towards the midline causing a lengthening and narrowing of the embryo) is important during neural tube

closure as without these cellular movements the neural folds are too far away from the midline and cannot fuse.

1.1.3. Mouse models of neural tube defects

Human NTDs are usually non-syndromic with complex genetic and environmental causative factors (multifactorial) (Juriloff et al. 1989; Sadler 2005). However, in mice more than 100 spontaneous or induced mutations in single genes have been shown to cause NTDs including spina bifida, exencephaly, craniorachischisis and split face (Boyles et al. 2005). The most common NTD associated with any single gene mutation in mice is exencephaly; for example, in *Ephrin-A5* (*Efna5*) and *Eph-A7* (*Epha7*) mutant mice (Holmberg et al. 2000). However, several mutant mouse models develop both exencephaly and spina bifida (*Shroom* [*Shrm*] (Hildebrand and Soriano 1999; Haigo et al. 2003) and *Cyp26A1 (Sakai et al. 2001)* mutant mice), a few mutants develop spina bifida alone (*Axial defects* [*Axd*] mutant mice) (Copp et al. 2003) and fewer develop craniorachischisis (*Lp* and *Crc* mutant mice) (Copp et al. 2003; Murdoch et al. 2003). These mouse mutants highlight the fact that different areas of the neural tube have unique molecular signals critical for closure in that region. However, the fact that some mutants have more than one associated NTD points to overlapping molecular signals along the length of the neural tube as well.

An interesting observation associated with some mutant mouse models such as *Splotch* (*Sp*) (Fleming and Copp 2000), *opb* (Gunther et al. 1994) and *curly tail* (*ct*) (van Straaten and Copp 2001) is that they can have different phenotypes and varying phenotypic penetrance and severity depending on the genetic background. In addition, some mouse genetic backgrounds such as NZW (Vogelweid et al. 1993), SWV/Bc and

CBA/Ca (Fleming and Copp 2000) already appear to have a higher probability of developing exencephaly than others (Harris and Juriloff 1999; Greene and Copp 2005). Teratogens may also have varying effects on NTD development depending on mouse genetic background. The variation in mice is usually in the development of cranial NTDs as opposed to caudal NTDs. The variation in closure point 2 on different genetic backgrounds is one of the causes hypothesized to infer a susceptibility to develop NTDs in the cranial region (Fleming and Copp 2000). Therefore, it is likely that there are gene variants in different mouse genetic backgrounds that may influence the development of cranial NTDs. If these modifying alleles are identified they may lead us to genetic factors which put humans at risk of developing cranial NTDs.

Although neurulation in mouse and humans may not be identical, mouse models have been used to study genes which may cause susceptibility to developing NTDs in humans as well as highlight pathways that are important in neural tube closure (Boyles et al. 2005). In general, human NTDs are perinatally lethal and approximately 80% arise with no other detectable defects (non-syndromic) (Harris and Juriloff 1997; Copp et al. 2003; Boyles et al. 2005; Sadler 2005).

Therefore, one problem with mouse models is that many mutant embryos die before birth due to other developmental defects (Harris and Juriloff 1997). Mutations which cause NTDs in mice and death *in utero* usually have other abnormalities. Therefore, it is difficult to determine if the NTD is directly caused by faulty neurulation or is a secondary effect due to other defects (Copp et al. 2003). Before these genes or molecular pathways are considered candidates for susceptibility to NTDs in humans, the mouse mutants that develop NTDs and die *in utero* must be carefully studied to ensure that the NTD is

caused by the gene mutation and is not a secondary effect of other developmental problems. For example *Sp/Sp* mutant mice develop extensive exencephaly and spina bifida and also have neural crest defects. Death in homozygous mutant embryos occurs between 12.5 and 16.5 dpc (Goulding et al. 1993). If it were not for the other neural crest defects associated with this mutation the homozygous mutant embryos would likely be carried to term and die around the time of birth.

A second problem with the use of mouse models to study human NTD susceptibility is that many mutations cause only exencephaly in mice. These genes and molecular pathways are then considered as potential candidates for susceptibility to all NTDs in humans. However, the mutation or pathway involved only affects cranial neurulation in mice. This is because spina bifida is not always lethal in humans, whereas anencephaly is. Therefore, it is easier to collect samples from spina bifida patients but more difficult to collects samples from anencephalic infants. Although cranial and caudal neurulation have overlapping molecular signals, there are unique signalling pathways as well. By studying mutant mouse models which exhibit only exencephaly, only spina bifida and those that develop both exencephaly and spina bifida, it will be easier to understand the unique and overlapping molecular signals that lead to these different phenotypes. Once molecular signals are determined it will be easier to understand some of the complex genetic interactions in humans that lead to the development of the different types of NTDs.

1.1.4. Cranial and caudal neural tube closure

As described above cranial and caudal neural tube closure likely have unique molecular signals as well as some overlapping signals. Some of these signals, or the

result of these signals, have been determined in mice. For example, the MHP is common to cranial and caudal neurulation. It is formed along the length of the ventral neural tube by Shh signalling from the notochord. In the upper spinal region, only the MHP exists and the neural tube develops a narrow lumen. The neural folds elevate and the tips bulge out slightly before fusion (Copp et al. 2003).

There are also two dorsolateral hinge points (DLHPs) that develop symmetrically in the cranial neural tube and the intermediate and lower spinal region (Copp et al. 2003; Sadler 2005). The molecular signals to develop the DLHPs in the cranial region are unknown at this time (Copp et al. 2003). However, in the intermediate and lower spinal region decreased Shh signalling appears to play a role in DHLP formation. Therefore, Shh may also play a role in cranial DHLP formation (Copp et al. 2003). If Shh signalling is indeed responsible for the formation of DLHPs in both the cranial and caudal regions, perhaps Shh is one of the overlapping signals important for cranial and caudal neurulation. Processes such as apoptotic regulation and retinoic acid signalling can cause exencephaly and spina bifida, indicating that these pathways may also have similar overlapping signals along the entire length of the neuroectoderm (Harris and Juriloff 1999).

Mesenchymal cell proliferation and microfilament contraction at the apical surface of cells in order to change the shape of the neural folds from convex to concave has been shown to be important in cranial neural tube closure (Copp et al. 2003). Actin must accumulate at the top of the cranial neuroectoderm cells and microfilament contractions create the DLHPs by causing the cells to become pie shaped. This allows the neural tube to bend and the neural folds to make contact and fuse. Therefore, gene mutations that

compromise the integrity of the cytoskeleton and mesenchymal proliferation have been studied for their ability to cause cranial NTDs in mice. For example, *Twist* and *Cart1* mutants have reduced amounts of cranial mesenchyme and only develop exencephaly. *MARCKS*, *RhoGAPp190* and *Vinculin* mutants all have cytoskeletal defects and only develop exencephaly (Copp et al. 2003). Therefore, mesenchymal cell proliferation and microfilament contraction may be unique molecular pathways involved in only cranial neurulation. Using single gene mouse mutants, more of the overlapping and unique molecular signals of neural tube closure are being discovered. As more information is gained, this knowledge of the molecular signals can then be used to study susceptibility genes in humans.

Genes that have been found to have a role in chromatin remodelling have been shown to cause exencephaly. Examples include *ATRX* (*α-thalassemia/mental retardation, X-linked syndrome*), *Brg1* (*Brahma related gene one*), *Smarcc1* (*SWI/SNF related, matrix associated, actin dependent regulator of chromatin, subfamily c, member 1*) (reviewed in Copp et al. 2003) and *Cecr2* mouse mutants (Banting et al. 2005). As these proteins are all likely involved in the regulation of other genes, determining how they are affecting cranial neurulation could answer more questions as to the molecular regulation of neural tube closure.

1.2. Chromatin remodeling

1.2.1. Chromatin remodelling: an overview

Chromatin is important for packaging eukaryotic DNA. Chromatin is made up of repeating nucleosome units of DNA wrapped around histone octamers (Johnson et al. 2005). Chromatin structure in eukaryotes can regulate many processes such as gene

expression, DNA replication, recombination, transcription, heterochromatin formation and DNA repair (Barak et al. 2004; Eberharter and Becker 2004; Johnson et al. 2005). Therefore, remodelling chromatin structure can be important for up or down regulating gene expression or other processes listed above. Chromatin can be remodelled by relocating or altering the structure of nucleosomes or covalently modifying histones and is therefore loosely defined as any process that alters the nuclease sensitivity of chromatin (Aalfs and Kingston 2000). In eukaryotic organisms, there are two classes of complexes that can remodel chromatin structure: histone modifying enzymes and ATP-dependent chromatin remodelling factors (Aalfs and Kingston 2000).

ATP-dependent chromatin remodelling factors are conserved among a wide variety of eukaryotic organisms with complexes in yeast, flies, frogs, mice and humans. They are therefore likely to be important for normal cellular activities and embryonic development (Fazzio et al. 2005). Within the ATP-dependent chromatin remodelling factors there are seven different families related through their ATPase domains: ISWI, SWI/SNF, CHD/Mi-2, INO80, RAD54, CSB and DDM1 (Eberharter and Becker 2004; Fazzio et al. 2005). The most common families are mating type switching/sucrose non-fermenting (SWI/SNF) and imitation switch (ISWI) (Aalfs and Kingston 2000). All of these families remodel chromatin in a variety of ways including altering histone-DNA contacts, assembling or disrupting nucleosomes, sliding of nucleosomes or exchanging histones within existing nucleosomes in regions where they are targeted (Fazzio and Tsukiyama 2003).

Chromatin remodelling proteins have been associated with several human disorders including ATRX (Hendrich and Bickmore 2001). ATRX syndrome in humans is

characterized by severe mental retardation, facial anomalies, variable degrees of urogenital defect, α-thalassemia and epileptic seizures. The ATRX protein has a SWI/SNF ATPase domain and PHD finger. It has been found to be part of a large multiprotein chromatin remodelling complex in human cells (Berube et al. 2002). When human ATRX is overexpressed in mice, they show similar phenotypes to humans with mutations in the ATRX gene. The mice show retarded growth, NTDs, brain growth and organization abnormalities, seizures, craniofacial anomalies, behavioural abnormalities and frequent embryonic and perinatal death (Berube et al. 2002). This data indicates that ATRX is likely dosage sensitive and too much or too little leads to the phenotypes listed above. As ATRX is a part of a chromatin remodelling complex, it is likely that ATRX dosage affects the activity of the complex that it is associated with, which in turn likely affects the expression of the genes with which the complex interacts (Berube et al. 2002). As this is not the only example of a chromatin remodelling complex involved in a human disease, it is not unlikely that other chromatin remodelling complexes may be involved in other unidentified human developmental disorders (Hendrich and Bickmore 2001).

1.2.2. The ISWI and SWI/SNF families

ISWI complexes were first discovered in *Drosophila* and SWI/SNF complexes were first identified in yeast (Aalfs et al. 2001; Johnson et al. 2005). Some of the major differences between the ISWI and SWI/SNF families are their complex size, subunit composition, substrate specificity and biochemical activity. ISWI complexes are much smaller (200-700 kDa) than SWI/SNF complexes (~2 MDa) and only have two to six protein components compared to SWI/SNF complexes, which can have eight to sixteen protein subunits (Aalfs et al. 2001; Johnson et al. 2005). ISWI complexes always contain

a protein homologous to *Drosophila* ISWI and usually contain another protein(s) that have PHD fingers (a zinc finger like domain that binds DNA), bromodomains (binds acetylated histones) (Grune et al. 2003; Johnson et al. 2005) and/or BAZ domains (a protein binding domain important in formation of the ACF complex) (Jones et al. 2000a; Eberharter and Becker 2004; Johnson et al. 2005). SWI/SNF complexes, on the other hand, always contain a yeast SWI2/SNF2 ATPase homologue that also has a bromodomain (Aalfs et al. 2001).

The SWI/SNF family ATPase activity can be stimulated by the presence of nucleosomes or naked DNA, whereas ISWI ATPase activity is only stimulated by nucleosomes (Aalfs and Kingston 2000). It is hypothesized that this is due to the chromatin remodelling role these different complexes have. ISWI complexes likely associate with nucleosomes to make a more mobile nucleosome structure whereas SWI/SNF complexes bind strongly to DNA to move the histones and increase access to the DNA (Aalfs and Kingston 2000). Biochemically, the ISWI family can slide and assemble nucleosomes, disrupt chromatin, alter nucleosome spacing (sliding) and disrupt chromatin assembly activities (Aalfs et al. 2001). The SWI/SNF family can alter the nuclease sensitivity of both mononucleosomes and linear arrays of nucleosomes, transfer histone octamers to non-adjacent DNA, create stable dinucleosomes from mononucleosomes and cause topological stress to naked DNA (Aalfs et al. 2001).

1.2.3. SNF2L containing complexes

In humans and mice, there are two ISWI homologues: SNF2L/Snf2l (SWI/SNF related, matrix associated, actin dependant regulator of chromatin, subfamily a, member 2) and SNF2H/Snf2h (SWI/SNF related, matrix associated, actin dependant regulator of

chromatin, subfamily a, member 5) (Barak et al. 2003). Many complexes have been identified in humans that contain the SNF2H protein including WSTF-related chromatin-remodelling factor (WCRF), ATP-utilizing chromatin assembly and remodelling factor (ACF), Remodelling and spacing factor (RSF), WSTF-ISWI chromatin-remodelling complex (WICH), Nucleosome-remodelling complex (NoRC), Chromatin assembly complex (CHRAC) and SNF2H-cohesin (Barak et al. 2003). However, until recently no complexes containing SNF2L had been identified.

The first complex in humans shown to form with SNF2L is human Nucleosome-remodelling factor (hNURF) (Barak et al. 2003). NURF had previously been identified as an ISWI complex in *Drosophila*. NURF contains three protein subunits in humans (four in *Drosophila*) including SNF2L, bromodomain PHD finger transcription factor (BPTF) and retinoblastoma-associated protein 48/46 (RbAp48/46). The ATPase activity of hNURF is stimulated by nucleosomes and to a small degree by naked DNA. The complex is enriched in the brain and increases the expression of human *engrailed 1* and *2*. NURF also has been shown to have a role in stimulating neurite outgrowth, which marks a developmental switch from dividing neuroblasts to terminally differentiated neurons (Barak et al. 2004).

Ramin Shiekhattar's laboratory at the Wistar institute in Pennsylvania has recently described a second SNF2L containing complex that forms between SNF2L and cat eye syndrome chromosome region, candidate 2 (CECR2). This new complex has been named the CECR2-containing remodelling factor complex (CERF complex) (Banting et al. 2005). CERF remodels chromatin in an ATP dependent fashion and is stimulated by

the presence of nucleosomes but not naked DNA. Therefore, CERF is a member of the ISWI family of ATP-dependent chromatin remodelling factors.

1.2.4. Possible CERF complex functions

Human NURF regulates the expression of *engrailed* (Barak et al. 2003). *Engrailed* is a homeodomain protein that regulates neuronal development in the mid-hindbrain regions. SNF2L has elevated expression in the brain and the reproductive organs. SNF2L likely plays other developmental roles in neuronal development and in reproductive organ development in mice and humans (Lazzaro and Picketts 2001). It is therefore probable that CERF has a role in neuronal and reproductive organ development.

1.3. CECR2/Cecr2

1.3.1. Chromosomal location

The McDermid lab has been researching the *CECR2* gene as part of their study of the rare developmental disorder cat eye syndrome (CES) (Footz et al. 2001). CES is caused by duplication (three or four copies) of a 2 Mb region on chromosome 22q11 in humans. Phenotypes include coloboma, ear tags and pits, anal atresia, kidney, skeletal and heart defects, and mental retardation. The phenotypes associated with CES are variable between patients. The *CECR2* gene (GenBank accession no. Q9BXF3) is located within the 2 Mb Cat Eye Critical Region on chromosome 22 in humans and in the region of conserved synteny on chromosome 6 in mouse (*Cecr2*) (Footz et al. 2001). It is predicted that one or more of the genes in the cat eye critical region may be dosage sensitive and extra copies of these genes may be responsible for some or all of the phenotypes detected in CES patients (Footz et al. 2001). *CECR2* was chosen as a good

candidate for a dosage sensitive role in CES, as preliminary analysis of the genomic and protein sequences indicated it may have a role in gene regulation.

1.3.2. CECR2/Cecr2 potential function

A previous graduate student, Graham Banting, was studying the potential role that *CECR2* may have in CES. He determined the *CECR2/Cecr2* gene has 19 exons and is characterized by a DDT domain (DNA binding homeobox and different transcription factors domain), adenine/thymine hook (AT hook), putative nuclear localization signal (NLS), and bromodomain **(Figure 2)** (Banting et al. 2005) .

DDT domains are predicted to bind to DNA (Doerks et al. 2001) and/or proteins. In *Drosophila melanogaster* it has been shown that the DDT domain of the Acf1 protein is necessary for Acf1 to bind to ISWI. This binding happens when forming the ACF complex *in vitro* (Fyodorov and Kadonaga 2002). AT hook motifs bind to the minor groove of double stranded DNA (Reeves and Nissen 1990; Aravind and Landsman 1998) and bromodomains have been shown to bind to acetylated lysine residues in the basic patch of histone H4 tails (Grune et al. 2003; Johnson et al. 2005). Bromodomains are also present in most histone acetyltransferase proteins (Dhalluin et al. 1999; Jones et al. 2000b). The motifs discussed so far support the Shiekhattar lab's finding that CECR2/Cecr2 has a role in chromatin remodelling as part of the CERF/CeRF complex. Proteins that remodel chromatin must be targeted to the nucleus and CECR2/Cecr2 contains a putative nuclear localization signal. Orr Barak, a collaborating researcher, has also predicted that CECR2 may contain a BAZ1 motif (Banting et al. 2005). BAZ1 motifs are important for protein interactions between ACF1 and SNF2H, a mammalian ISWI homologue, forming the ACF complex (Jones et al. 2000a).

1.4. Phenotype associated with *Cecr2* mutation

As CECR2/Cecr2 was thought to be a dosage sensitive protein involved in gene regulation, a *Cecr2* mutant mouse model was created by Graham Banting (Banting 2003). The mutation within the *Cecr2* gene is caused by a genetrap insertion within intron 7 (Tate et al. 1998; Banting et al. 2005). The genetrap is a splicetrap that should create a fusion protein between the first seven exons of the *Cecr2* gene and the *lacZ* gene coding sequence. The mutant allele has been named $Cecr2^{Gt45Bic}$ (Banting et al. 2005).

Sixty-seven percent of BALB/129P2 mice homozygous for this mutation develop the cranial neural tube defect exencephaly with no other detectable phenotypes **(Table 3 see results section)**. Non-penetrant weaned mice with closed neural tubes appeared normal. Therefore, it appears that Cecr2 is involved in cranial neurulation. It may control the expression of other genes important during cranial neural tube closure by remodelling chromatin in the promoter regions of such genes.

The penetrance of exencephaly in homozygous $Cecr2^{Gt45Bic}$ mutants is variable depending on mouse genetic background. In an experiment not related to the work described above, FVB/N mice were mated to BALB/129P2 mice carrying the $Cecr2^{Gt45Bic}$ mutation. The penetrance of exencephaly in $Cecr2^{Gt45Bic}$ homozygous mutant mice on this new mixed genetic background (BALB/129P2/FVB) dropped to 36% **(Table 3 see results section)**. To analyse the effect mouse genetic background has on the penetrance of exencephaly, it was decided to move the $Cecr2^{Gt45Bic}$ mutation onto 3 pure genetic backgrounds: BALB/c, 129P2/ola and FVB/N, which is one of the goals of this study.

A small proportion of $Cecr2^{Gt45Bic}$ heterozygotes also exhibited the exencephaly phenotype (3.5% on the BALB/129P2 background and 4% on the BALB/129P2/FVB

background) **(Table 3 see results section)**. This lends further evidence that *Cecr2* is dosage sensitive. Since a reduction in the expression of *Cecr2* leads to a developmental defect, it would also be interesting to investigate the effect of overexpressing the same protein. Therefore, CECR2, when overexpressed, is still a good candidate for CES as it is very likely dosage sensitive. Further investigation into the phenotypes that might be associated with overexpression of this gene will shed light on what developmental roles CECR2 may have in CES.

1.5. Research objectives

The research objectives of the current study focus on how genetic background affects the penetrance of the exencephaly phenotype, analysis of *Cecr2* expression at the approximate time of neural tube closure, and the creation of an anti-Cecr2 antibody for further analysis of Cecr2 in development. These objectives were analyzed as follows:

1. To create incipient congenic BALB/c, FVB/N and 129P2/ola mouse genetic backgrounds carrying the $Cecr2^{Gt45Bic}$ mutation and analyze the penetrance of exencephaly on each genetic background.
2. To analyze the male/female ratio of the exencephaly phenotype on different mouse genetic backgrounds.
3. To confirm that the Cecr2-lacZ fusion protein expression is the same on the BALB/c genetic background as it was on the BALB/129P2 genetic background.
4. To examine *Cecr2* expression at the time of neural tube closure using the Cecr2-lacZ fusion protein at 9.5 dpc.
5. To create and analyze anti-Cecr2 antibodies using Western blot analysis.

6. To confirm Cecr2 protein is expressed in homozygous mutant mouse tissues as previous RT-PCR data suggests (Banting 2003).

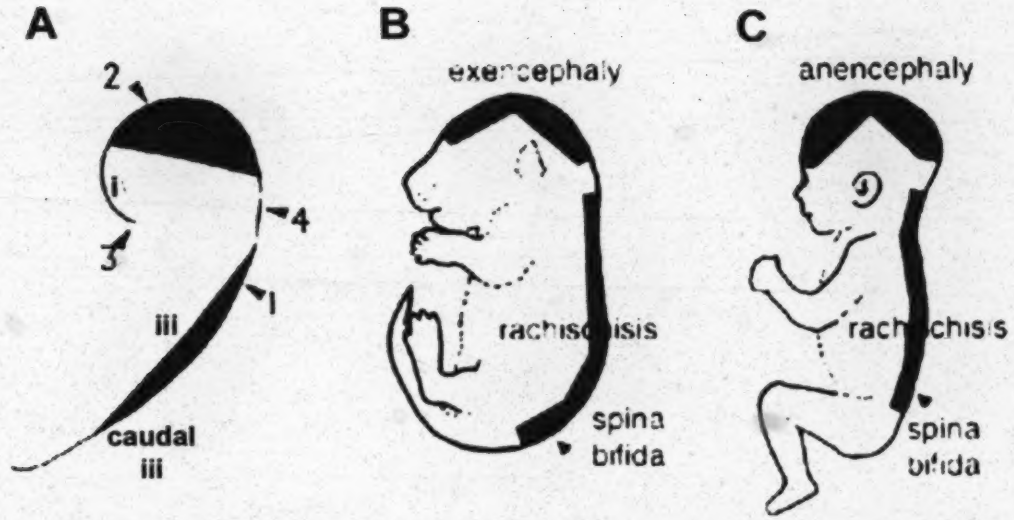

Figure 1. Schematic diagram of the four neural tube closure points and the associated NTD phenotype. Location of the four contact points are indicated by an arrowhead and numbered in order of occurrence (A). If the area between contact points does not close properly into a tube then an NTD develops. For example if the red area ii (A) fails to close, then the NTD exencephaly (B) or anencephaly (C) will develop in mice and humans respectively. This diagram is published in *Hum. Mol. Gent.* by Juriloff and Harris 2000.

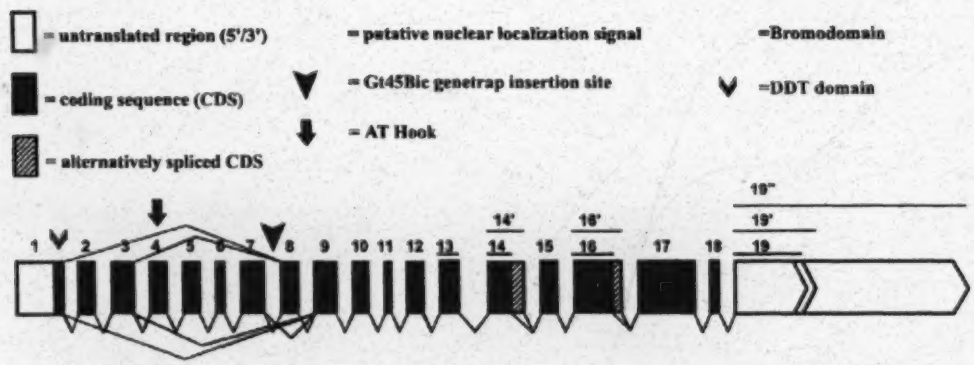
= untranslated region (5'/3')
= coding sequence (CDS)
= alternatively spliced CDS
= putative nuclear localization signal
= Gt45Bic genetrap insertion site
= AT Hook
=Bromodomain
=DDT domain
1 2 3 4 5 6 7 8 9 10 11 12 13 14' 14 15 16' 16 17 18 19" 19' 19

Figure 2. Schematic diagram of the mouse *Cecr2* gene. The exons are drawn to scale however, the introns are not. Relevant motifs are illustrated. The alternative splicing shown is predicted based on sequence results obtained from RT-PCR on human tissues. The splicing out of exon 8 has been confirmed in multiple mouse tissues. The existence of exons 14 and 14' has also been confirmed in mice. Adapted from Banting 2003.

Chapter 2. Materials and Methods

2.1. Mouse colony upkeep

2.1.1. Mouse housing

The mouse colony was housed at the University of Alberta's Health Sciences Laboratory Animal Services (HSLAS). Mice were housed in standard filter top cages with no more than five mice per cage. They were supplied a constant source of water and food (Laboratory Rodent Diet 5001 from LabDiet). Pregnant dams were fed a higher fat content food throughout pregnancy and lactation (Mouse diet 9F 5020 from LabDiet). The animals were kept at 22 ± 2°C and on a 14 hour light 10 hour dark cycle. Animals were checked everyday by HSLAS staff and at least once per week by the McDermid lab and euthanized if any illness occurred.

2.1.2. Mouse breeding

Male mice were mated with individual females or harems of up to four females. If a harem was set up, the females were removed to an individual cage once they were visibly pregnant. Males were occasionally left in with individually housed females to encourage post partum mating. Once a litter was born the pups remained with the female for three weeks at which point they were weaned by an HSLAS staff member. The pups were then ear notched and a tail biopsy was taken by the McDermid lab for identification and genotyping purposes, respectively.

When embryos at a specific developmental stage were required, one male with up to four females were placed together between noon and 6pm. The next morning the females were checked by HSLAS staff for the presence of a vaginal plug left by the male during copulation. If a plug was found the female was removed from the cage. The plug day

was counted as 0.5 days post coitum (dpc) for calculation of gestational age. The mouse was euthanized using CO_2 at the appropriate gestational age and the embryos dissected.

2.1.3. Euthanasia

Mice were euthanized in a standard CO_2 chamber and monitored for at least 10 minutes after death was thought to have occurred. They were tested for pain response via toe pinching before being placed in a freezer until incineration.

2.2. Embryo manipulation

2.2.1. Embryo dissection

Embryos were dissected in 1x PBS (137 mM NaCl, 2.7 mM KCl, 10 mM Na_2HPO_4 and 2 mM KH_2PO_4 pH 7.4) under approximately 12 x magnification on a dissecting microscope. Extraembryonic membranes were removed and used for DNA isolation and genotyping. If embryos were needed for RNA or protein extraction, the dissection was carried out at the HSLAS facility in 0.1% DEPC treated 1x PBS. The tissue was placed directly into RNase free tubes and frozen on dry ice as quickly as possible. Prior to dissecting, all tools were treated with 10% SDS or 0.1 M NaOH. All 9.5 dpc embryos were dissected under the dissecting microscope at the McDermid lab.

2.2.2. X-gal staining

Embryos at 9.5-13.5 dpc were dissected from timed pregnant dams euthanized by CO_2. They were placed into 1.5 (9.5 dpc) or 2.0 ml (>9.5 dpc) Eppendorf tubes, washed once with 1x PBS, and then fixed at 4°C for 1-2 hours in 4% paraformaldehyde/0.1% DEPC treated 1x PBS. Fixed embryos were then washed 3 x 5 minutes in at least 500 µl of 1x PBS followed by 3 x 15-30 minute washes in *LacZ* wash solution (2 mM $MgCl_2$, 0.01% deoxycholic acid and 0.02% IGEPAL in 0.1% DEPC treated 1x PBS pH 7.2 stable

for up to one year). The embryos were then stained at 37°C in freshly prepared *LacZ* stain solution (2 mM $MgCl_2$, 0.01% deoxycholic acid, 0.02% IGEPAL, 5 mM potassium ferricyanide, 5 mM potassium ferrocyanide and 1 mg/ml X-gal in 0.1% DEPC treated 1x PBS pH 7.2) until desired stain intensity was reached. Following a variable staining time ranging from one hour to overnight, the process was stopped by washing 3 x 5 minutes with 1x PBS. Embryos were photographed at this point or dehydrated in a methanol (MeOH) gradient for long term storage at -20°C (5 minute washes in 25%, 50% and 75% MeOH in 1x PBS followed by 3 x 5 minute washes in 100% MeOH) (Banting 2003).

2.3. Nucleic acid isolation

2.3.1. Mouse genomic DNA isolation

Mouse genomic DNA was isolated from three sources: mouse tail biopsies, embryo biopsies or extraembryonic membranes. The samples were incubated overnight at ~60°C in 350 µl of proteinase K digestion buffer (50 mM Tris pH 8, 100 mM EDTA pH 8 and 0.2% SDS) and 300 µg of proteinase K (Invitrogen). Samples were then removed from the water bath and placed on ice for 5 minutes, followed by the addition of 125 µl of 5 M NaCl (~1.7 M final concentration). The tubes were placed on ice for an additional 5 minutes and then centrifuged in a microcentrifuge, with a fixed angle rotor, for 15 minutes at 14 000 rpm. The supernatant was added to new tubes with 500 µl of isopropanol and 0.75 µl of 2% dextran blue (to visualize the pellet). The new tubes were placed at -20°C for at least 30 minutes and then centrifuged for 15 minutes at 14 000 rpm. The pellets were rehydrated with 500 µl of 70% ethanol (EtOH) and centrifuged again for 15 minutes at 14 000 rpm. The EtOH was decanted and the pellets dried before the DNA was resuspended in 20 µl of dH_2O (Banting 2003; Maier 2005). To isolate DNA from

9.5 dpc mouse embryo extraembryonic membranes the protocol was modified as follows. Extraembryonic membrane samples were added to 300 µl of proteinase K digestion buffer and 250 µg of proteinase K and then treated the same as described above.

2.3.2. DNA extraction from agarose gels

PCR amplified DNA to be sequenced was cut from 1-2% agarose gels and placed into pre-weighed 1.5 ml Eppendorf tubes. The DNA was then isolated as per manufacturer's instructions using a QIAkit gel extraction kit (250) (Qiagen). An aliquot of the extracted DNA was electrophoresed on a 1% agarose gel to determine the approximate concentration of the DNA sample.

2.3.3. RNA isolation

RNA was extracted using TRIzol reagent (Invitrogen) modified from manufacturer's instructions. An Ultra-Turrax homogenizer was used to homogenize 100 to 200 mg of tissue with 1 ml of TRIzol. The samples were incubated at room temperature for 5 minutes and then centrifuged at 4°C in a microcentrifuge, with a fixed angle rotor, for 10 minutes at 11 000 rpm. The supernatant was added to 200 µl of chloroform, incubated at room temperature for 3 minutes, and centrifuged again at 4°C for 15 minutes. The upper aqueous phase was added to an equal volume of ice cold isopropanol, incubated at room temperature for 10 minutes, and centrifuged again for 15 minutes at 4°C. The pellet was then washed in 1 ml of ice cold 75% EtOH (diluted in 0.1% DEPC treated water) followed by centrifugation for 10 minutes at 4°C. The RNA pellet was dried for approximately 5 minutes and resuspended in 50-100 µl of 0.1 % DEPC treated water. The concentration and purity of the samples were tested using the Genesys 10 UV spectrophotometer (Thermo Electron Corporation) at 260 and 280 nm.

2.4. PCR

2.4.1. RT-PCR

A 10 µl volume containing approximately 1 µg of total RNA, extracted using the TRIzol method described above, as well as 1 U of DNaseI (Invitrogen) in 1x DNaseI reaction buffer (Invitrogen) and 40 U of RNaseOUT (Invitrogen) were incubated for 15 minutes at room temperature. The enzymatic reactions were stopped with 1 µl of 25 mM EDTA and incubation at 65°C for 10 minutes. First strand cDNA synthesis was then performed using the ThermoScript RT-PCR System (Invitrogen) as per manufacturer's instructions. The above mixture was added to 1x cDNA synthesis buffer, 5 mM DTT, 1 mM dNTPs, 20 pmol of a gene specific primer (Cecr2 10eR1 or CECR2 R11) **(Table 1)** and 12 U ThermoScript reverse transcriptase. The samples were then incubated in the PTC-100 thermal cycler (MJ Research) with the following cycling conditions: 42°C for 30 minutes, 50°C, 54°C, 58°C, 62°C and 65°C for 10 minutes each, and 85°C for 5 minutes. The samples were incubated for 20 minutes at 37°C with 2 U of RNase H and stored at -20°C for up to one month. A 1:4 dilution of cDNA was used as the template for PCR amplification as described below. As a negative control for each RNA sample, the same procedure was followed with the omission of the ThermoScript reverse transcriptase.

2.4.2. Sequencing reactions

Sequencing reactions (half-reaction volume of 10ul) were performed using the DYEnamic ET terminator cycle sequencing kit (Amersham Biosciences) modified from the manufacturer's instructions. Each half-reaction contained 4.5 µl of PCR product (approximately 50 ng of DNA), 2 pmol of the appropriate primer, 4 µl of sequencing

premix, and 0.5 µl of 2% dextran blue. The samples were then cycled 30 times as follows: 96°C for 30 seconds, 60°C for 1 minute and 50°C for 1 minute. DNA was precipitated by adding 1 µl of 1.5 M NaOAc/250mM EDTA pH >8 and 40 µl of 95% EtOH followed by 30 minutes at -20°C. The samples were centrifuged in a fixed angle rotor microcentrifuge at 14 000 rpm for 15 minutes and the EtOH was decanted. The DNA was washed in 200 µl of 70% EtOH and centrifuged again at 14 000 rpm for 5 minutes. The pellet was then dried for 5 minutes and taken to the Molecular Biology Service Unit (MBSU) in the Department of Biological Sciences at the University of Alberta where it was resuspended in formamide loading dye and run on an ABI 377 automated sequencer (Applied Biosystems).

2.4.3. PCR reactions

PCR amplification was performed using a 25 µl reaction volume in a PTC-200 thermal cycler (MJ Research) as follows. Each reaction contained 1 µl of the appropriate concentration of DNA template, 10 pmol of each primer, 1x PCR buffer (25 µM Tris pH9, 50 µM KCl, 1.5 µM $MgCl_2$ and 0.02 mg/ml bovine serum albumin (BSA) dissolved in DEPC treated water), 0.2 mM dNTPs (Invitrogen) and 1 U (0.5 µl) of recombinant *Taq* DNA polymerase (purified by Dr. Pickard in the Department of Biological Sciences, University of Alberta). The reactions were then cycled as follows: a "hotstart" of 94°C for 1 minute and 30 seconds followed by holding at 80°C until the *Taq* polymerase was added, then 35-50 cycles of 94°C for 15 seconds, the appropriate primer annealing temperature (usually 60-62°C) for 20 seconds, 72°C for 1 minute per Kb of amplification and one final extension step at 72 °C for 5 minutes. The primer annealing temperature

was chosen to be 5-10°C below the Tm of the primer calculated using the formula Tm= 67.5 + 34(%gc)-(395/#bp) (Stephanie Maier personal communication).

2.4.4. *Cecr2*^{Gt45Bic} mutation genotyping PCR

A multiplex PCR, designed by Graham Banting, was used to check sex and genotype mice for the presence of the *Cecr2*^{Gt45Bic} mutation (Banting et al. 2005). The following five primers were used in this PCR: Cecr2 7iF4, Cecr2 7iR4, pGT1 R4, SRY Fwd, and SRY Rev **(Table 1)**. These primers can amplify up to three bands per DNA sample **(Figure 3)**. A 376 bp fragment within intron 7 of wild type *Cecr2* allele is amplified by Cecr2 7iF4/R4 (please note Cecr2 7iF1/R1 published in Banting 2003 and Banting et. al. 2005 are not the correct primers for genotyping mice with the *Cecr2*^{Gt45Bic} as they do not flank the genetrap insertion site, Cecr2 7iF4/R4 are the correct primers). This primer pair cannot amplify the mutant allele as they flank the insertion site of the genetrap within intron 7, which is approximately 6100 bp. The mutant allele is amplified by Cecr2 7iF4/pGT1 R4 and produces a 573 bp band. The SRY Fwd/Rev pair amplifies a 266 bp fragment in the *SRY* gene of male mice **(Figure 3)** (Banting et al. 2005). Undiluted genomic DNA extracted from mouse tail biopsies, embryo biopsies or extraembryonic membranes as described above was used as the template in the PCR reactions. Each 20 µl PCR reaction contained the following: 1 µl of DNA (approximately 0.5 µg of DNA), 20 pmol of each primer (Cecr2 7iF4, 7iR4, pGT1 R4, SRY Fwd and Rev), 1x PCR buffer, 0.25 mM dNTPs and 1 U (0.5 µl) of recombinant *Taq* DNA polymerase added to each well after a "hotstart". The PCR reactions were performed in PCR plate wells with an overlay of mineral oil in each well to prevent evaporation. The cycling conditions were as follows: a "hotstart" of 94°C for 1 minute and 30 seconds followed by

holding at 80°C until the *Taq* polymerase was added then, 35 cycles of 94°C for 15 seconds, 62°C for 20 seconds and 72°C for 40 seconds, and one last extension step at 72°C for 5 minutes. The samples were then kept at 4°C until the products were electrophoresed on an agarose gel. One times loading dye (50% glycerol, 10 mM Tris pH 7.5, 100 mM EDTA, 0.1% bromophenol blue, 0.1% xylene cyanol and 0.1% orange G) was added to each PCR reaction and the samples were electrophoresed on a 2% agarose gel at ~130 V for at least 45 minutes. EtBr (0.5 µg/ml) was added to the agarose gel to visualize the DNA using UV light. For each genotyping PCR reaction, four template controls were included as follows: wild type, heterozygous, homozygous *Cecr2*^{Gt45Bic} mutant mouse DNA as well as water. Each gel included a lane of 1 Kb plus DNA ladder (Invitrogen) to size the bands.

2.5. Characterizing the *Cecr2*^{Gt45Bic} mutation on BALB/c, FVB/N and 129P2/ola genetic backgrounds

2.5.1. Congenic line production

Previously, Dr. Peter Dickie at HSLAS produced a chimera by blastocyst injections into C57BL/J6 mouse blastocysts. Dr. Dickie performed blastocyst injections using 129P2/ola derived CT45 ES cell line (Tate et al. 1998) provided by Dr. Wendy Bickmore (MRC Human Genetics Unit, Edinburgh). This ES cell line carries a splicetrap mutation within intron 7 of the *Cecr2* gene (*Cecr2*^{Gt45Bic}=*m*) (Banting 2003). The chimera produced from these injections was mated to normal BALB/c females to create a BALB/129P2 genetic background of mice carrying the above described mutation in the *Cecr2* gene.

In an experiment unrelated to any of this work, these BALB/129P2 mice were mated to FVB/N mice to produce a BALB/129P2/FVB genetic background carrying the *Cecr2*^{Gt45Bic} mutation. Homozygous mutant mice developed the NTD exencephaly (Banting 2003). However, the penetrance of this phenotype differed significantly between the two mixed genetic backgrounds, appearing in 67% of the mutant BALB/129P2 mice and 36% of the mutant BALB/129P2/FVB mice **(Table 3 see results section** and Banting et al. 2005). To investigate the penetrance of the exencephaly phenotype on pure genetic backgrounds, the *Cecr2*^{Gt45Bic} mutation was moved from the BALB/129P2/FVB mixed genetic background onto BALB/c, 129P2/ola and FVB/N pure genetic backgrounds.

2.5.2. Penetrance data collection

The penetrance of exencephaly was investigated on incipient congenic lines of all three genetic backgrounds at generations F4 to F6 (http://www.jax.org/imr/controls.html). An incipient congenic line of mice is any genetic background that has been backcrossed to a pure strain less than ten times. After five backcrosses the incipient congenic line is approximately 90% genetically identical to the backcross strain (Juriloff et al. 1989; http://www.jax.org/imr/controls.html). At the appropriate generation, heterozygous mice of the same genetic background were intercrossed to produce enough heterozygous mice of each strain to harvest approximately 200 embryos. Once enough mice were produced, heterozygous mice of the same genetic background were plug tested to confirm copulation had occurred. Embryos were then harvested between 12.5 and 19.5 dpc and scored for exencephaly. Technician Amanda Campbell and myself genotyped the

embryos for *Cecr2*^{Gt45Bic} using DNA extracted from extraembryonic membranes or embryo biopsies as described above.

2.6. Anti-Cecr2 antibodies

2.6.1. Anti-Cecr2 pep A, B, C and D production

Four peptides were selected within the mouse Cecr2 protein sequence as follows: Cecr2 pep A amino acids (aa) 68-78 (YQRRDITPQTF), Cecr2 pep B aa 764-773 (NGNHGTTNPG), Cecr2 pep C aa 1003-1012 (DTYKTSKNKN) and Cecr2 pep D aa 1282-1296 (DWQRSLPSQR) **(Table 2)**. Particular attention was paid to choose a peptide on the outside of the native Cecr2 protein to increase the antigenic properties of the peptide. Therefore, hydrophobic regions, regions of secondary structure, cysteine and methionine residues, homopolymers as well as post-translationally modified amino acids were avoided (manual May 10, 2001). The Alberta Peptide Institute made and conjugated each peptide to both the KLH (keyhole limpet hemocyanin) and BSA proteins. Each KLH conjugated peptide was injected three times into two separate rabbits by Biological Laboratory Animal Services (BSLAS) staff. The rabbits and the antigen they were injected with are as follows: Cecr2 pep A into rabbit 2I1 and 2I2, Cecr2 pep B into 2G2 and 2G3, Cecr2 pep C into 2I6 and 2I7, and Cecr2 pep D into 2G6 and 2I4. The first injection incorporated Freund's complete adjuvant (Sigma) and the subsequent two injections incorporated Freund's incomplete adjuvant (Sigma). The injections each contained ~0.5 mg of the appropriate peptide KLH conjugate dissolved in 900 µl of 1x PBS and 900 µl of Freund's complete or incomplete adjuvant. A 5 ml syringe was used with a 1.5 inch 22 gauge needle to mix the two components. Before any injections were given, 5 ml of pre-immune serum from each rabbit was collected.

injection the BSLAS staff provided blood for testing of anti-Cecr2 antibody titer. After three months each rabbit was exsanguinated and serum was collected for further testing.

2.6.2. Protein extraction

Total protein extracts from mouse tissues were isolated using a RIPA buffer kit (Boehringer Mannheim) as per manufacturer's instructions. The tissue was washed 2 x 5 minutes in ice-cold 1x PBS. The tissue was then homogenized using an Ultra-Turrax homogenizer in RIPA buffer (50 mM Tris, pH 7.5, 150 mM NaCl, 1% Nonidet-P40, 0.5% sodium deoxycholate, 0.1% SDS and a complete mini protease inhibitor cocktail tablet [Roche]) at a concentration of 100 mg of tissue per ml of buffer. The samples were then centrifuged at 14 000 rpm for 10 minutes at 4°C in a fixed angle rotor microcentrifuge to remove any debris. The protein supernatant was quantified and stored at -70°C.

A DC assay kit (BioRad) was used to quantify the protein concentrations as per manufacturer's instructions. Known concentrations of BSA were used as the protein standards. Each sample contained 20 µl of protein combined with 100 µl of reagent A and 800 µl of reagent B. The samples were left for 15 minutes before the absorbance at 750 nm was recorded using the Genesys 10 UV spectrophotometer. A standard curve was produced using the known BSA standards and the A_{750} readings of the protein samples of interest were used to determine the concentration values.

2.6.3. Western blot using nitrocellulose membrane

One millimeter SDS-PAGE gels for protein electrophoresis were made as follows: separating gel layer contained 7.5% acrylamide, 375 mM Tris pH 8.8, 1% SDS, 0.1% APS, and 10 µl of TEMED (Invitrogen); stacking gel layer contained 4% acrylamide,

125 mM Tris pH 6.8, 1% SDS, 0.1% APS, and 2.5 µl TEMED. The protein samples were made as follows: the appropriate amount of total protein extract was added to a 1x final concentration of SDS loading dye (58 mM Tris pH 6.8, 1.7% SDS, 5% glycerol, 100 mM DTT and 10 mM bromophenol blue) up to a final volume of 12 µl and boiled for 1.5 minutes (Maier 2005). These samples were loaded along with BenchMark protein ladder (Invitrogen) into the stacking gel. The gels were run in 1x SDS running buffer (25 mM Tris, 192 mM glycine and 0.1% SDS) at 50 mA for approximately 2 hours using a Hoefer SE 600 series gel electrophoresis apparatus (Amersham Biosciences). The proteins were then electroblotted onto Hybond-ECL nitrocellulose membrane (Amersham Biosciences) at 75 mA overnight at 4°C using the Hoefer Transphor apparatus (Amersham Biosciences). The transfer buffer contained 25 mM Tris, 192 mM glycine, 0.1% SDS and 20% MeOH (Maier 2005). The membranes were then stained using 1x Ponceau S (Sigma) to visualize the transferred proteins. The excess Ponceau was washed away with 5% acetic acid and the protein markers were traced with a pencil. The Ponceau stain was then removed by washing for 15 minutes with PBS-Tween (81 mM Na_2HPO_4, 25 mM NaH_2PO_4, 625 mM NaCl and 0.1% Tween-20). The membranes were then blocked in 5% blotto (Carnation skim mild powder in PBS-Tween) for at least one hour and then washed 2x quickly and 2 x 2 minutes with PBS-Tween. They were then incubated with the primary antibody of interest (anti-Cecr2 pep A, C and D serum antibodies) diluted 1:2000 in 5% blotto for at least 1.5 hours. The membranes were then washed 2x quickly and 4 x 5 minutes with PBS-Tween. Secondary antibody (goat F(ab')2 Anti-Rabbit IgG (H+L) HRPO conjugate [Caltag Laboratories]) was diluted 1:5000 in 5% blotto and incubated with the membranes for at least 45 minutes. The

membranes were then washed with PBS-Tween 2x quickly and 4 x 5 minutes (Maier 2005). An ECL kit (Amersham Biosciences) was used to visualize the HRPO signal according to package instructions on BioMax XAR film (Kodak) exposed for 20 minutes to overnight.

2.6.4. Affinity purification

Anti-Cecr2 pep A, C and D antibodies were affinity purified using CNBr-activated Sepharose 4B beads (Pharmacia Biotech) according to package instructions. The beads were prepared for antigen coupling by swelling 0.6 g per column in 25 ml of 1 mM HCl. The beads were placed in a sintered glass filter hooked up to a vacuum flask. They were then washed in 6 ml aliquots of 1 mM HCl for 15 minutes followed by 10 minutes of washing with 5 ml aliquots of coupling buffer (0.1 M $NaHCO_3$ pH 8.3 and 0.5 M NaCl). The beads were centrifuged in a swinging bucket clinical centrifuge at 800 x g for 1 minute and the supernatant was removed. To conjugate, 7.5-15 mg of each BSA-Cecr2 peptide of interest dissolved in coupling buffer (ligand) was incubated overnight at 4°C with 1.5 ml of Sepharose beads. The slurry was centrifuged at 600 x g in a swinging bucket clinical centrifuge for 5 minutes at 4°C. Excess ligand was removed by alternating 4 times between 5 minute washes with 2.5 ml of cold coupling buffer and 5 minutes spins at 600 x g. The remaining active sites on the Sepharose beads were blocked by 4-5 hour incubation at 4°C with 3 ml of cold 0.1 M Tris pH 8. The slurry was then poured into a poly prep column (BioRad) avoiding air bubble formation. The column was washed with 3 cycles of 10 ml acetate wash pH 4 (0.1 M NaOAc and 0.5 M NaCl) and 10 ml Tris wash pH 8 (0.1 M Tris and 0.5 M NaCl). These washes were followed by 3 x 2 ml washes with ice cold 1x PBS. During all nine of the above washes,

the drip rate was one drip every 3-6 seconds. Three-hundred micro liters of the appropriate clarified antiserum was loaded onto the column followed by the addition of 0.3 ml of 1x PBS. The column was left for 1 hour to allow the anti-Cecr2 antibody to bind to the ligand. Another 0.3 ml of 1x PBS was added, collected, and recycled through the column four times. The column was then washed with 5 x 2.5 ml of cold 1x PBS. The purified antibody was then eluted by adding 6 ml of elution buffer pH 2.3 (50 mM glycine and 0.1 M NaCl) 1 ml at a time and collecting each fraction into 0.2 ml of 1 M Tris pH 8. The column was then washed with 4 x 5 ml ice cold 1x PBS. The fractions were concentrated into ~1.5 ml using Amicon ultra-15 centrifugal filter device 15-30 000 MW (Millipore) and stored at -20°C. The columns were stored at 4°C in 20% EtOH/1x PBS until further use.

2.6.5. Western blot using PVDF membrane

SDS-PAGE gels, at a thickness of 0.75 mm, for protein electrophoresis were made as follows: separating gel layer contained 6-10% acrylamide, 420 mM Tris pH 8.8, 0.1% SDS, 0.07% APS, and 8 µl TEMED; stacking gel layer contained 5% acrylamide, 62.5 mM Tris pH 6.8, 0.1% SDS, 1.2% APS, and 10 µl TEMED. The protein samples were made as follows: the appropriate amount of total protein extract was added to a 1x final concentration of SDS loading dye up to a final volume of 12 µl and boiled for 5 minutes. These samples were loaded along with BenchMark protein ladder into the stacking gel. The gels were run in 1x SDS-PAGE running buffer (25 mM Tris, 190 mM glycine and 0.1% SDS pH 8.3) at 200 V for approximately 1 hour using a mini-protean 3 cell gel electrophoresis apparatus (BioRad). The proteins were then electroblotted onto Immobilon-P PVDF membrane (Millipore) at 100 V for 1.5 hours or 30 V overnight at

4°C using the mini-protean 3 cell transfer apparatus (BioRad). The transfer buffer contained 25 mM Tris, 190 mM glycine and 20% MeOH. The membranes were then stained using 1x Ponceau S to visualize the transferred proteins. The excess Ponceau stain was washed away with 5% acetic acid and the proteins markers were traced with a pencil. The Ponceau stain was then removed by washing for 15 minutes with PBS-T (0.1% Tween-20 in 1x PBS). The membranes were then blocked in 5% milk solution (Carnation skim mild powder in PBS-T) for at least 1 hour at room temperature or overnight at 4°C and then washed 3 x 5 minute with PBS-T. They were then incubated for at least 1 hour with either anti-Cecr2 pep A purified antibody diluted 1:500 or anti-Cecr2 pepC antibody diluted 1:1000 in 2.5% BSA (Sigma)/PBS-T. The membranes were then washed 2x quickly, 1 x 10 and 1 x 5 minutes with high salt PBS-T (HSPBS-T: 0.1% Tween-20 and 500 mM NaCl in 1x PBS). Secondary antibody (goat F(ab')2 anti-rabbit IgG (H+L) HRPO conjugate) was diluted 1:5000 in 2.5% BSA in HSPBS-T and incubated with the membranes for at least 30 minutes. The membranes were then washed with PBS-T 2x quickly and 2 x 5 minute. An ECL kit was used to visualize the HRPO signal according to package instructions on BioMax XAR film exposed for 5-20 minutes.

2.6.6. Competition assay

To determine if the bands produced using anti-Cecr2 pep A and C antibodies were specific, two competition assays were performed. In each assay, BSA conjugated to the appropriate peptide, BSA alone, adult mouse liver and brain total protein extracts, as well as BenchMark protein ladder were electroblotted onto PVDF membrane as described above. The amount of each sample for the pep A competition was as follows: 100 ng of BSA-pep A, 100 ng of BSA alone, 20 µg of liver and 50 µg of brain. The amount of

each sample for the pep C competition was as follows: 50 ng of BSA pep C, 50 ng of BSA alone and 7.5 µg of liver and brain. For each competition assay, 6 membranes with the above mentioned samples were used. The 6 primary antibodies used for detection of Cecr2 on each of the PVDF membranes were as follows: pre-immune serum from the rabbit of interest, purified antibody from the rabbit of interest, purified antibody from the rabbit of interest incubated with 10x or 50x excess of the appropriate peptide conjugated to BSA, and purified antibody from the rabbit of interest incubated with 10x or 50x excess of BSA alone. Each of the six samples described above was incubated at 37°C for 1-2 hours and then left overnight at 4°C to allow the antibody to bind to the antigen. The samples were then centrifuged at 4°C for 15 minutes at 14 000 rpm to remove any antibody-antigen conjugates. The supernatant was then diluted in 2.5% BSA PBS-T as follows: 1:1000 for pep A 2I1 pre-immune, 1:1500 for pep A 2I1 purified, 1:2000 pep C 2I6 pre-immune and 1:1000 pep C 2I6 purified. Using the diluted supernatants as primary antibodies, the procedure was then the same as described above for Western blot detection on PVDF membrane.

Table 1. Primer sequences used in this study

Primer Name	Location	Sequence 5' to 3'[a]
CECR2 F21	*H. sa. CECR2* exon 1	gcc atc gcg cac ttc tgc tc
Cecr2 7iF4	*M. mu. Cecr2* intron 7	Ccc cat tta ttt gct tga gct g
Cecr2 7iR4	*M. mu. Cecr2* intron 7	cac gaa caa tgg aag gaa tga
CECR2 R11[a]	*H. sa. CECR2* exon 10	gct ttc tcc tct tcg ctc gat
Cecr2 10eR1	*M. mu. Cecr2* exon 10	gct ttc tcc tct tag ctc gat
SRY Fwd	*M. mu. SRY* gene	gag agc atg gag ggc cat
SRY Rev	*M. mu. SRY* gene	cca ctc ctc tgt gac act
pGT1 R4	pGT1 genetrap vector	acg cca tac agt cct ctt cac atc

[a]Grey shaded area is not identical between human and mouse *Cecr2* sequence.

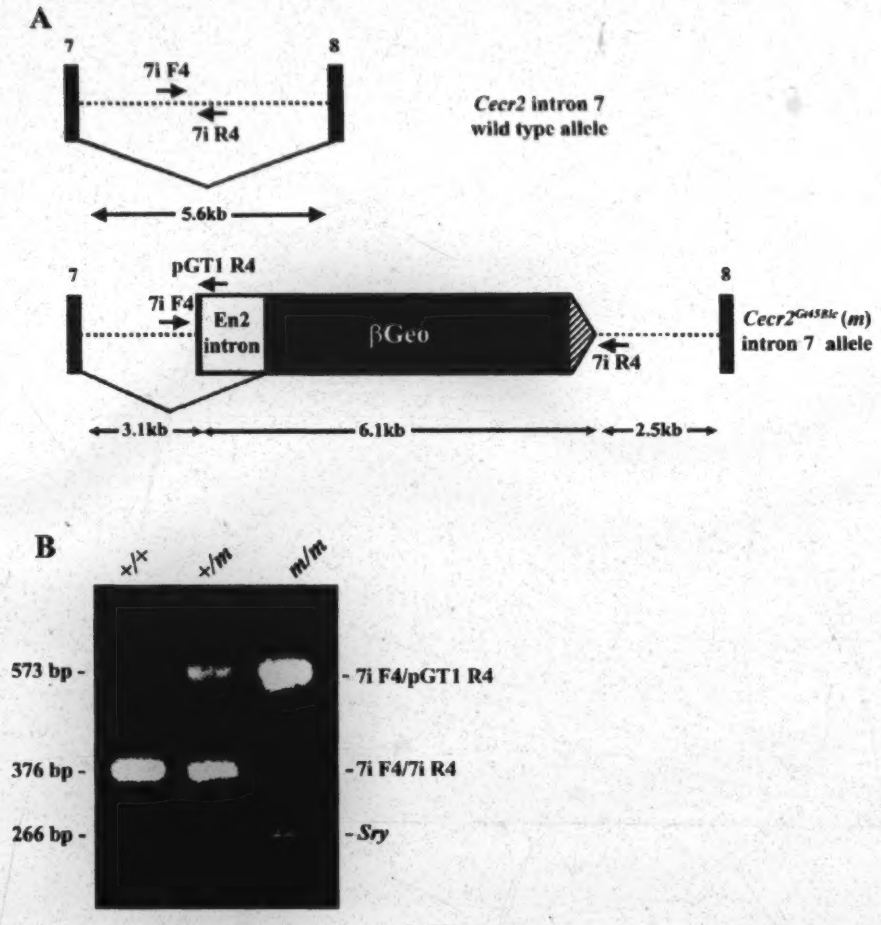

Figure 3. Location of the *Cecr2*^{Gt45Bic} genetrap within *Cecr2* intron 7 and a sample genotyping PCR gel electrophoresis picture. *Cecr2* intron 7 wild type and *Cecr2*^{Gt45Bic} mutant allele and location of the 3 primers used for mouse genotyping (A). Sample picture of the three potential products amplified in the *Cecr2*^{Gt45Bic} genotyping PCR. The largest band at 573 bp corresponds to the mutant allele and the 376 bp band corresponds to the wild type allele. The *Sry* band at 266 bp is amplified by male specific SRY Fwd and SRY Rev primers annealing to the male *Sry* gene. No product at this size indicates the mouse is female. Note these primers are not indicated on the diagram in A. Figure adapted from Banting, 2003.

Table 2. Location of Cecr2 peptides used in the production of anti-Cecr2 antibodies.

Peptide name	Location in full length mouse Cecr2 protein	Amino acid sequence[a]	Identity to human CECR2
Cecr2 pepA	68-78	YQRRDITPQTF	100%
Cecr2 pepB	764-773	NGNHGTTNPG	80%
Cecr2 pepC	1003-1012	DTYKTSKNKN	50%
Cecr2 pepD	1282-1296	DWQRSLPSQR	70%
Cecr2 pepWB	1420-129	PVQSQSLFPK	80%

[a]Grey shaded areas are areas that differ between human and mouse Cecr2 protein sequence.

Chapter 3. Results

3.1. The penetrance of exencephaly differs depending on mouse genetic background

Previous work using the *Cecr2*^{Gt45Bic} mutation indicated that mouse strain may affect the penetrance of the exencephaly phenotype in homozygous mutant mice. Graham Banting determined the penetrance of exencephaly in homozygous mutants on the BALB/129P2 mouse genetic background to be 67% **(Table 3)**. In an unrelated experiment, FVB/N mice were mated to BALB/129P2 mice carrying the *Cecr2*^{Gt45Bic} mutation. The penetrance of exencephaly in homozygous mutant embryos on this new BALB/129P2/FVB genetic background dropped significantly (χ^2 test for independence, p=0.004) to 36% **(Table 3)**. Graham Banting and I both collected this penetrance data. To investigate how genetic background affects the frequency of the exencephaly phenotype, the *Cecr2*^{Gt45Bic} mutation was moved onto BALB/c, 129P2/ola and FVB/N genetic backgrounds.

Cecr2^{Gt45Bic} heterozygous BALB/129P2/FVB mice were mated to wild type BALB/c, 129P2/Ola and FVB/N mice to move the mutation from the mixed genetic background onto the three pure genetic backgrounds of interest **(Figure 4)**. This mating created the F1 generation of each of the new lines, which were genotyped using a multiplexed PCR designed by Graham Banting **(Figure 3)**. Mice heterozygous for the *Cecr2*^{Gt45Bic} mutation were chosen and mated to the same wild type genetic background as in the parental cross to create the next generation. To create congenic lines this process was repeated for the BALB/c and FVB/N strains for at least ten generations. The 129P2/ola strain was only taken to incipient congenic status at generation F5 due to mismothering by most females of this genetic background **(Figure 4)**.

To collect penetrance data for each background, *Cecr2*$^{+/Gt45Bic}$ mice of all three strains were intercrossed at generations F4 through F6 to produce enough mice to investigate the penetrance of the exencephaly phenotype associated with the mutation **(Figure 5 A-C)**. The penetrance of exencephaly was investigated on incipient congenic lines at generation F4 or greater. The penetrance of the exencephaly in homozygous mutants varied on each genetic background as follows: 74% on BALB/c, 63% on 129P2/ola and 0% on FVB/N **(Table 3)**. All of these values are statistically different from one another (χ^2 test for independence, $p=1.1 \times 10^{-12}$). In fact, all five strains investigated to date produce a different penetrance of the open neural tube phenotype (χ^2 test for independence, $p=3.1 \times 10^{-24}$).

3.2. Female mutant embryos develop exencephaly more frequently

All of the embryos harvested for observation of the exencephaly phenotype were scored for sex using PCR amplification of the SRY gene **(Figure 3)**. On BALB/c and BALB/129P2/FVB genetic backgrounds, the female embryos had a higher penetrance rate of exencephaly than the males **(Table 4)**. On the incipient congenic BALB/c genetic background, 88% of females compared to 57% of homozygous mutant males had exencephaly **(Table 4)**. These values are statistically significant (χ^2 test for independence, p-value of 0.01). The difference in the BALB/129P2/FVB genetic background is 52% of females and 23% of males develop exencephaly **(Table 4).** These values are also statistically significant (χ^2 test for independence, p-value of 0.02). The BALB/129P2 and 129P2/ola genetic backgrounds were not investigated as not all embryos in the BALB/129P2 genetic background were scored for sex and the number of embryos collected from the 129P2/ola genetic background was too small.

The male/female data was also analysed as the percent of male and female embryos that had exencephaly out of the total number of exencephalic embryos for a more direct comparison with previously reported data. On the BALB/129P2/FVB and BALB/c genetic backgrounds, out of all the exencephalic embryos, approximately 66% were female and 33% were male (χ^2 test for independence, p-value of 0.0007 and 0.001 respectively) **(Table 5)**.

3.3. *Cecr2*^{Gt45Bic} reporter gene expression on the incipient congenic BALB/c genetic background

The *Cecr2*^{Gt45Bic} genetrap mutation is a splicetrap located within the seventh intron of the *Cecr2* gene **(Figure 2)**. This splicetrap contains the coding region of the *LacZ* gene. This mutation should allow production of a fusion protein between the translated product of the first seven exons of *Cecr2* and the *LacZ* gene. Expression of the fusion protein should be under the control of the endogenous *Cecr2* promoter. Therefore, if embryos that are homozygous or heterozygous for the *Cecr2*^{Gt45Bic} genetrap are stained using X-gal, blue staining should be detected where endogenous *Cecr2* transcript may be located. Wild type embryos should not show any blue staining.

I used this fusion protein to my advantage to determine where endogenous *Cecr2* may be expressed at 12.5 dpc in BALB/c embryos. The tissues that stain at 12.5 dpc on a BALB/c genetic background **(Figure 5 D-F)** are similar to those that stained on the BALB/129P2 genetic background at 13.5 dpc performed by Graham Banting (data not shown) (Banting 2003). Cecr2 fusion protein can be seen in the brain, spinal column, spinal ganglia, eyes, nasal cavities and mesenchyme of the limbs in both genetic backgrounds and at both embryonic stages. The BALB/c 12.5 dpc wild type negative

control does show faint staining in the eyes and limbs **(Figure 5 G-H).** However, the staining pattern seen in the BALB/c 12.5 dpc heterozygous mouse is highly repeatable at different stages as well as on different genetic backgrounds, whereas the staining in the wild type eyes and limbs is not usually detected (data not shown). It is therefore likely that *Cecr2* is expressed in all of the tissues listed above.

3.4. *Cecr2*^{Gt45Bic} reporter gene expression just after neural tube closure on the BALB/129P2 genetic background

The only detectable phenotype in homozygous *Cecr2*^{Gt45Bic} mutant embryos is exencephaly. Therefore, I investigated the spatial distribution of the *Cecr2* transcript at the approximate time of neural tube closure, 9.5 dpc. I studied this using X-gal staining on 9.5 dpc embryos from the BALB/129P2 mixed genetic background. In both homozygous **(Figure 6 A and B)** and heterozygous **(Figure 6 C and D)** embryos an overall general staining pattern was seen. The staining was enriched in the developing neural tube and absent in the developing heart and liver. The open neural folds can be seen in the cranial region from the dorsal and lateral views of the homozygous mutant embryos **(Figure 6 A and B)**. The neural folds in heterozygous **(Figure 6 C and D)** and wild type **(Figure 6 E and F)** embryos are already fused. These BALB/129P2 embryos have therefore completely closed their neural tube at this point in gestation, indicating the mutant embryos with unfused neural folds would develop exencephaly if they were carried to term. The wild type littermate controls do not show any X-gal staining **(Figure 6 E and F)**.

3.5. *Cecr2* alternative splicing

There are many potential alternative splices within the first 10 exons of mouse *Cecr2* **(Figure 7).** These predicted splice sites are based on human RT-PCR performed by Graham Banting in 2003. I tested for the presence of the different predicted transcripts in various mouse tissues using RT-PCR. I began by amplifying *Cecr2* cDNA using CECR2 R11, a primer specific to human *CECR2* exon 10 **(Table 1)**. This primer is 95% identical to mouse *Cecr2* exon 10. I chose this human specific primer as Melanie Kardel, an undergraduate student in the lab, had been using this primer during her undergraduate project in both humans and mice and had shown promising results. I then PCR amplified from the cDNA template between exons 1 and 10 using CECR2 F21 and CECR2 R11 **(Table 1)**. CECR2 F21 is 100% identical to mouse exon 1. This PCR had the potential to produce six different bands corresponding to the six potential transcripts that could be made **(Table 6)**. In 12.5 dpc mouse embryo two bands were produced, corresponding to 982 bp and 1066 bp **(Figure 8)**.

A new strategy was taken by Courtney Davidson, an undergraduate summer student in the lab. Courtney amplified the cDNA with a redesigned CECR2 R11 primer called Cecr2 10eR1, which was 100% identical to mouse *Cecr2* **(Table 1)**. Exons 1-10 of this new cDNA were then PCR amplified with primers CECR2 F21 and Cecr2 10eR1. The new RT-PCR strategy was repeated on 12.5 dpc embryos as a positive control because it was known based on previous RT-PCR that two transcripts at 982 and 1066 bp should amplify from this sample. It was also performed on adult mouse brain and liver total RNA. In all samples, the same two bands at 1066 and 982 bp were seen as well as several smaller bands **(Figure 9)**. The bands at 1066 bp and 982 bp were confirmed by

sequencing to be complete *Cecr2* exons 1 through 10 and *Cecr2* exons 1 through 10 with exon 8 spliced out, respectively. Most of the smaller bands are not the correct size to be *Cecr2*. However, all three samples did contain a 600 bp band that may correspond to *Cecr2* exons 1-3 spliced to exons 8-10. None of these smaller bands produced useful sequence information so this cannot yet be confirmed. In all cases, the RT-PCR negative controls and the PCR water controls were blank **(Figures 8 and 9)**.

3.6. Creation of anti-Cecr2 antibodies

The Cecr2 protein was analyzed for potential secondary and tertiary structure using bioinformatics. Four peptides, predicted to be on the outside of the native Cecr2 protein, were selected for use in the production of anti-Cecr2 antibodies. Each peptide was approximately ten amino acids long. Bob Parker of the Alberta Peptide Institute also predicted ten peptides as good candidates for antibody production. These predictions were considered when determining the peptides to order. Peptides A, B, C and D were produced and conjugated to KLH carrier protein by the Alberta Peptide Institute **(Figure 10)**. These conjugates were then injected into rabbits to induce antibody production. An ELISA test was performed on all eight rabbits to determine if anti-Cecr2 antibodies were being made. Although this assay did not indicate that the rabbits were raising anti-Cecr2 antibodies, the injections continued and serum was collected for further testing.

3.7. Analysis of anti-Cecr2 peptide A, B, C and D antibodies

Several Western blots were performed on a series of mouse tissues using the appropriate peptide conjugated to BSA as a positive control. Anti-Cecr2 pep A, C and D serum detected an ~80 kDa band in the BSA-peptide positive control lanes **(Figure 11 and data not shown)**. This ~80 kDa band was not detected using anti-Cecr2 pep B

serum. Since it appeared that anti-Cecr2 pep B did not recognize its peptide, this serum was not tested further. The anti-Cecr2 pepC serum was tested for its ability to detect Cecr2 in adult mouse liver and brain whole protein extract. Two signals were detected at 160 kDa in liver and 140 kDa in brain **(Figure 11)**. This indicates that different isoforms of the Cecr2 protein may be expressed in a tissue specific manner.

The same conditions were used to determine the expression of the Cecr2 protein in wild type and *Cecr2*^{Gt45Bic} heterozygous and homozygous mutant adult mouse liver and brain whole protein extracts. The anti-Cecr2 pep C antibody was raised towards a C-terminal peptide, which is past the *Cecr2*^{Gt45Bic} genetrap. The genetrap should cease transcription within Cecr2 intron 7. Therefore, no protein signal should be detected in the homozygous mutant mouse tissues unless transcriptional read-through is occurring **(Figure 10 A)**. In all three genotypes of both adult mouse liver and brain signals at 160 and 140 kDa respectively were detected **(Figure 12)**.

The anti-Cecr2 pepA, C and D antibodies were affinity purified and tested for use in a competition assay to confirm their specificity. For each antibody the appropriate peptide conjugated to BSA was used as the positive control and BSA alone was used as the negative control. Adult mouse liver and brain samples were also loaded to test for the specificity of the 160 and 140 kDa signals. Unfortunately, a new aliquot of secondary antibody was used during these assays. As a result signals in adult liver and brain were now present in the pre-immune test **(Figure 13 D and 14 D)** and the sizes of the bands were different from previous tests (160 kDa in liver and 170 kDa in brain) **(Figure 13 and 14)**. This non-specific binding was attributed to the secondary antibody in further tests performed by Amanda Campbell as the bands were detected when only the

secondary antibody was used in the detection. However, in both anti-Cecr2 pepA and C competition tests, the peptide-BSA conjugate control signal was successfully competed away using a 10x and 50x excess of the peptide to antibody **(Figure 13 A,B and C and 14 A, B and C)**. A mock competition test using 10x and 50x excess of BSA alone was also performed and the peptide-BSA conjugate signal at ~80 kDa was not competed away **(Figure 13 E and F and 14 E and F)**. Anti-Cecr2 pepD was not tested in a competition assay. This data indicates that the affinity purified anti-Cecr2 pepA and C antibodies appear to have specificity for the peptides used to create them. Further testing must be done to determine their specificity in mouse tissues.

3.8. Analysis of anti-peptide WB antibodies

Washington Biotechnologies was also hired to develop an anti-Cecr2 antibody. They selected several peptides, approximately 15 amino acids long, predicted to be good antigens. A single peptide was selected near the C-terminal end of the Cecr2 protein (Cecr2 pepWB). This peptide was injected into two rabbits and several bleeds were taken and sent to me for testing. Western blot analysis was used to test this serum using peptide conjugated to carrier protein 39 (CP39), CP39 alone, and the C-terminal half of the CECR2 protein expressed in insect cells (Ctco#2) as controls (Ctco#2 control provided by Twila Yobb and Isabelle Mousseau). Faint signals were detected in the CP39-pepWB lane at ~40 kDa and in the Ctco#2 lane at ~110 kDa **(Figure 15)**. The CP39 alone and the pre-immune serum tested on the same three samples were blank **(Figure 15)**. As the signals were weak, the rabbits were boosted with pep WB antigen and the serum was then affinity purified by Washington Biotechnologies. This antibody

has not been tested on mouse tissue samples to date nor has a competition assay been performed. However, this work is being continued in the McDermid lab.

Table 3. The penetrance of exencephaly in *Cecr2*$^{Gt45Bic/Gt45Bic}$ mice is variable depending on mouse genetic background. [d]

Strain	BALB/129P2			BALB/129P2/FVB			FVB/N[a]			BALB/c[a]			129P2/ola[a]		
Genotype	*m/m*	*+/m*[b]	*+/+*	*m/m*	*+/m*	*+/+*	*m/m*	*+/m*	*+/+*	*m/m*	*+/m*	*+/+*	*m/m*	*+/m*	*+/+*
Exencephaly	24	4	0	21	7	1[c]	0	0	0	35	0	0	5	1	0
Normal	12	109	38	37	166	82	45	103	60	12	110	70	3	18	8
Penetrance (%)	67	3.5	0	36	4	1	0	0	0	74	0	0	63	5.3	0

[a]Data was collected from incipient congenic strains, mostly at generation F6 but with some at F5.

[b]*m* = *Cecr2*^{Gt45Bic}, + = wild type

[c]This is the only +/+ embryo out of 250 embryos scored that had exencephaly. No other wild type embryos in any other experiments have had exencephaly. Therefore, I have assumed this is a sporadic event.

[d]This table was published in Banting et al. 2005.

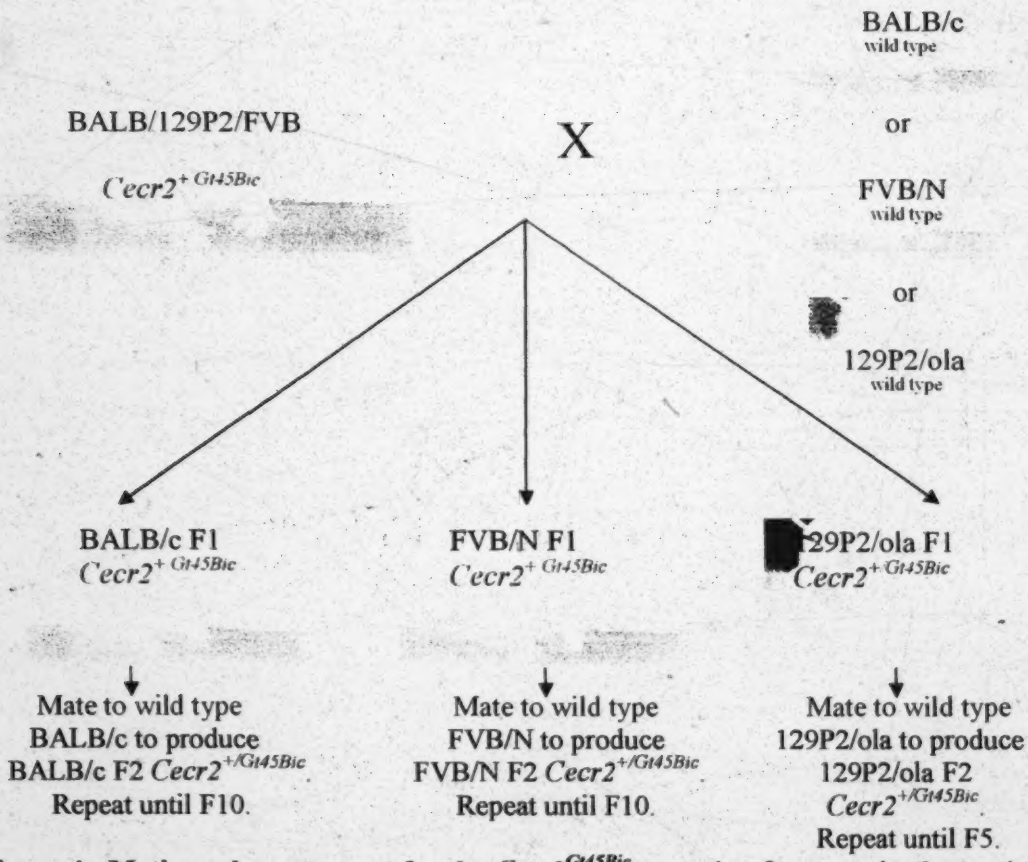

Figure 4. Mating scheme to transfer the *Cecr2*^{Gt45Bic} mutation from a mixed genetic background onto BALB/c, FVB/N and 129P2/ola genetic backgrounds. BALB/129P2/FVB mice heterozygous for the *Cecr2*^{Gt45Bic} mutation were mated to wild type mice of the three pure genetic backgrounds listed above. This produced F1 progeny for each genetic background of interest. The F1 progeny were then mated again to a wild type mouse of the same pure genetic background used in their parental cross to produce F2 mice. This process was repeated for at least ten generations to produce congenic BALB/c and FVB/N strains carrying the *Cecr2*^{Gt45Bic} mutation. The 129P2/ola strain was bred to generation F5 only, due to inherent breeding problems within the line. Each of the three lines was then analyzed for penetrance of the exencephaly phenotype.

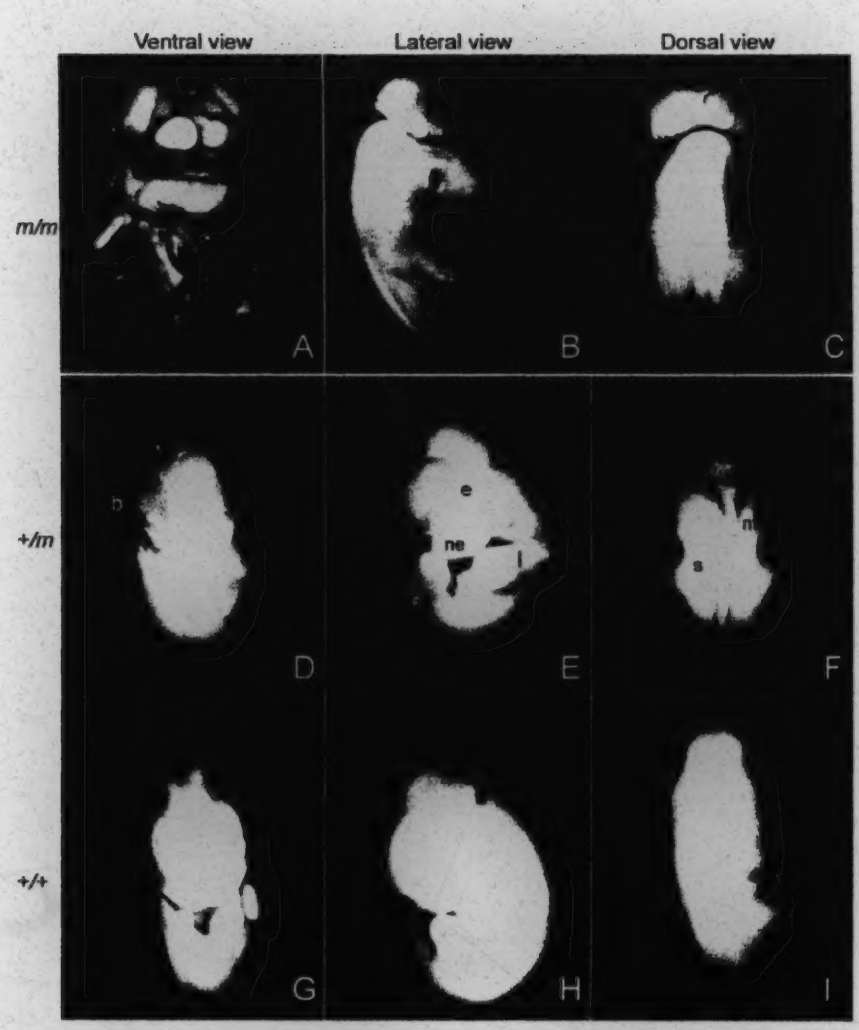

Figure 5. X-gal staining showing expression of the Cecr2-LacZ fusion protein in the congenic BALB/c genetic background. Homozygous mutant 13.5 dpc mouse embryo showing the exencephaly phenotype (A-C). Heterozygous 12.5 dpc embryo shows a similar expression pattern to the BALB/129P2 mice (D-F). X-gal staining is seen in the developing neural tube (nt), spinal ganglia (s), brain (b), nasal epithelium (ne), mesenchyme of the limbs (l) and eyes (e). Wild type littermates do show some weak staining in the limbs and eyes (G-H); however, this is uncharacteristic and not reproducible.

Table 4. Female embryos homozygous for the *Cecr2*^{Gt45Bic} mutation have a higher penetrance of exencephaly than males with the same homozygous mutation on two different genetic backgrounds.

Strain	BALB/129P2/FVB		BALB/c	
Genotype	*m/m*		*m/m*	
	♀	♂	♀	♂
Exencephaly	14	7	23	12
Normal	13	24	3	9
Penetrance (%)	52	23	88	57
p-value	0.02		0.01	

Table 5. Male/Female ratio of *Cecr2*^{Gt45Bic} mutant embryos with exencephaly

Strain	Percent (#) of exencephalic embryos		p-value
	♀	♂	
BALB/129P2/FVB	67% (14/21)	33% (7/21)	0.0007
BALB/c	66% (23/35)	34% (12/35)	0.001

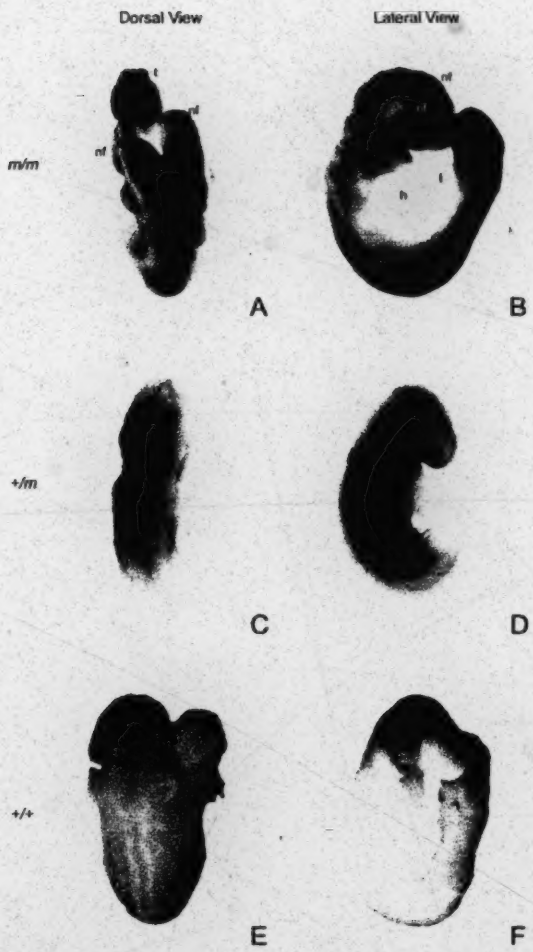

Figure 6. X-gal staining of 9.5 dpc mouse embryos showing expression of the Cecr2-LacZ fusion protein just after neural tube closure. The neural folds (nf) are not fused in *m/m* embryos (A and B). The heart (h) and liver (l) show no staining in m/m embryos (B). The dorsal and lateral views of homozygous mutant embryos shows general staining throughout the embryo with enriched staining in the open neural tube (A and B). The tail (t) can be seen in the dorsal view of the embryo. The heterozygous embryo shows the same staining pattern (C and D) as the homozygous mutant embryos (A and B). Wild type embryos show no staining (E and F). Please note these are not littermates therefore staining intensity may vary.

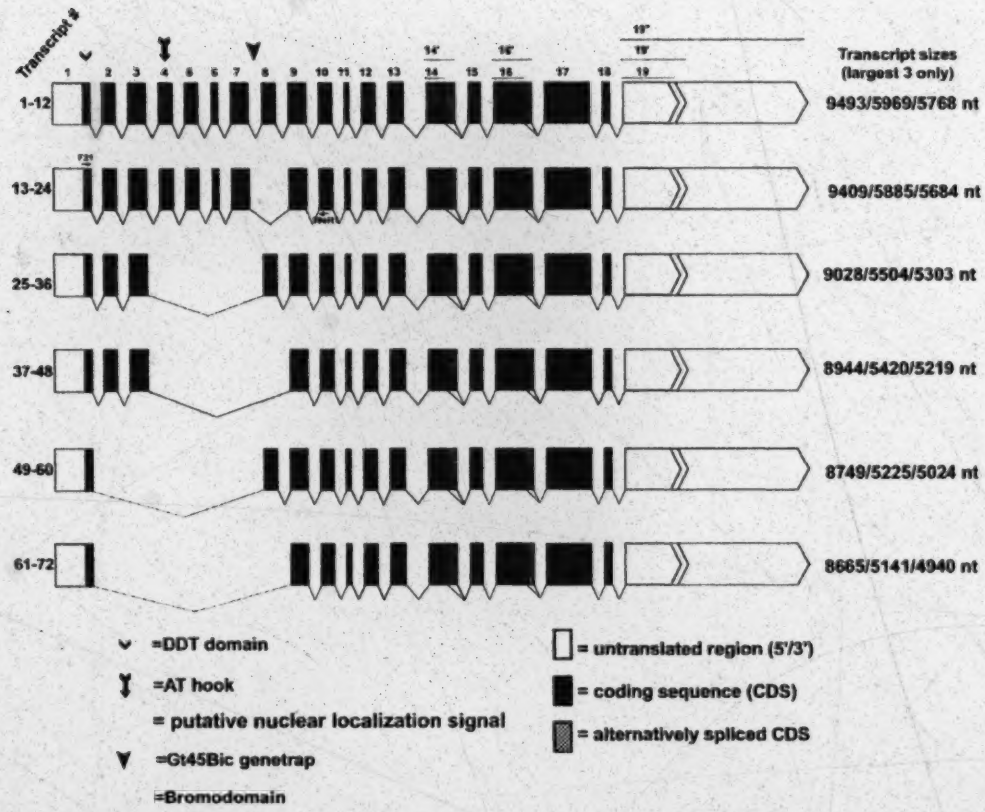

Figure 7. Potential alternatively spliced transcripts produced from the *Cecr2* gene. This subset of transcripts is based on RT-PCR performed in humans by Graham Banting. The splicing out of exon 8 in the full length transcript has been confirmed in multiple mouse tissues as well as mouse ESTs. The presence of exons 14 and 14' has also been confirmed. The remaining transcripts are predicted. Note that all potential transcripts contain both the DDT domain and bromodomain. These are critical domains for chromatin remodelling activity. (Adapted from Banting, 2003)

Table 6. Potential PCR products that can be produced from *Cecr2* cDNA using PCR primer sets CECR2 F21/CECR2 R11 or CECR2 F21/Cecr2 10eR1. These primer sets amplify between exons 1 and 10. These product sizes are predicted based on RT-PCR done by Graham Banting in human samples. The 1066 and 982 bp product sizes have been confirmed in multiple mouse tissues as well as mouse ESTs.

PCR product size (bp)	Corresponding Transcript (Included exons)
1066	1-10
982	1-7, 9-10
601	1-3, 8-10
517	1-3, 9+10
322	1, 8-10
238	1, 9+10

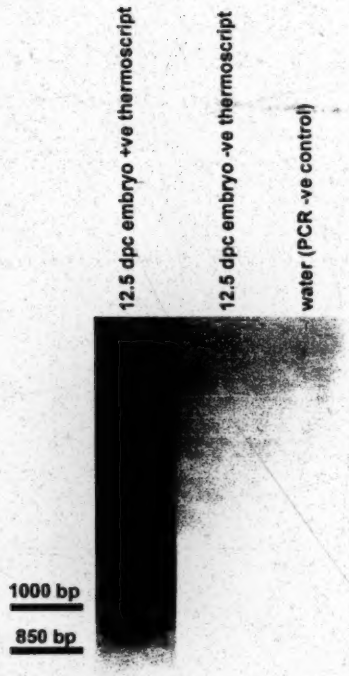

Figure 8. Expression analysis of *Cecr2* in 12.5 dpc embryo using RT-PCR. *Cecr2* cDNA was amplified using CECR2R11. The cDNA was then PCR amplified between exons 1 and 10 using primers CECR2 F21 and CECR2 R11. Table 3 indicates the potential product sizes and their corresponding transcripts. Two bands were detected at 982 bp and 1066 bp. Sequencing data from other RT-PCR experiments indicates the larger band to be *Cecr2* exons 1-10 and the smaller band to be *Cecr2* and exons 1-10 with 8 spliced out. The cDNA amplification negative control lane, where the thermoscript enzyme was not added to the reaction, is blank, as is the PCR water control.

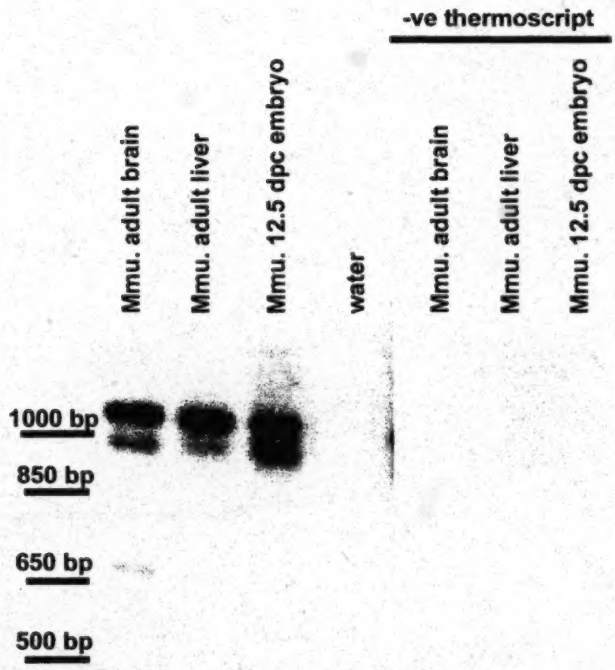

Figure 9. Expression analysis of *Cecr2* in adult mouse brain, liver and 12.5 dpc embryo using RT-PCR. *Cecr2* cDNA was amplified using Cecr2 10eR1. The cDNA was then PCR amplified between exons 1 and 10 using primers CECR2 F21 and Cecr2 10eR1. Table 3 indicates the potential product sizes and their corresponding transcripts. All three tissues show bands at 982bp and 1066 bp. Sequencing confirmed the larger band to be *Cecr2* exons 1-10 and the smaller band to be *Cecr2* and exons 1-10 with exon 8 spliced out. The smaller bands (all under 850 bp) only produced unreadable sequence data likely due to multiple overlapping PCR products at that size. However, the band seen at 600 bp is of interest as it is the correct size for exons 1-3 spliced to exons 8-10. The cDNA amplification negative control lanes, where the thermoscript enzyme was not added to the reaction, is blank as is the PCR water control. This RT-PCR was performed by Courtney Davidson, an undergraduate student in the lab.

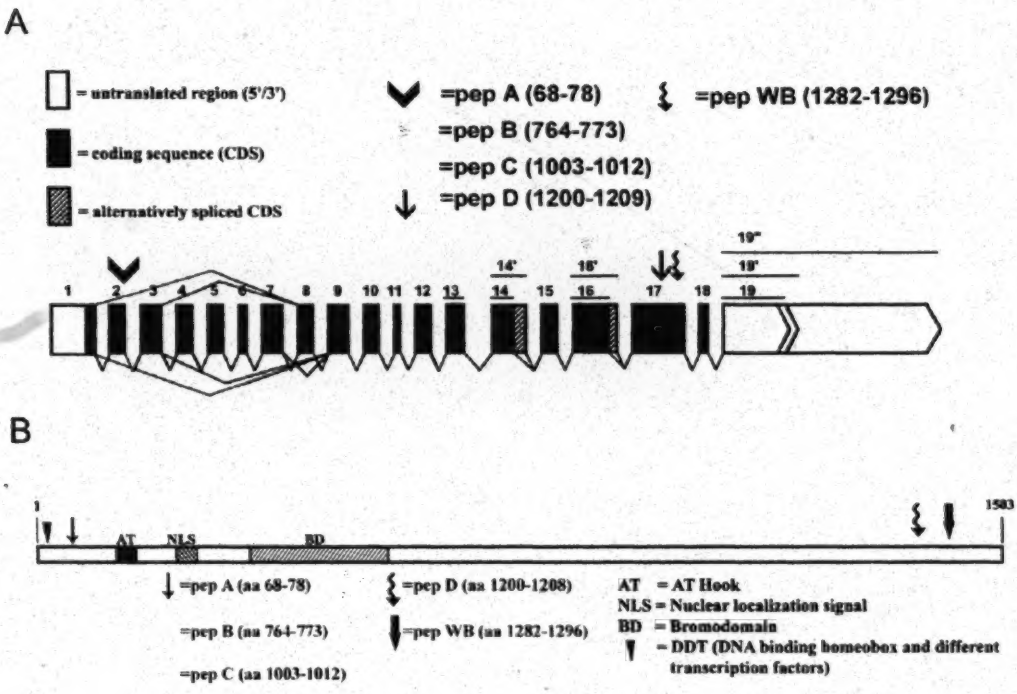

Figure 10. Location of the anti-Cecr2 epitopes. Shown are schematics of the Cecr2 gene (A) and the Cecr2 protein (B) and the locations of five antibodies raised towards peptides within the Cecr2 protein. The amino acid numbers of the peptides are indicated in brackets after the antibody name.

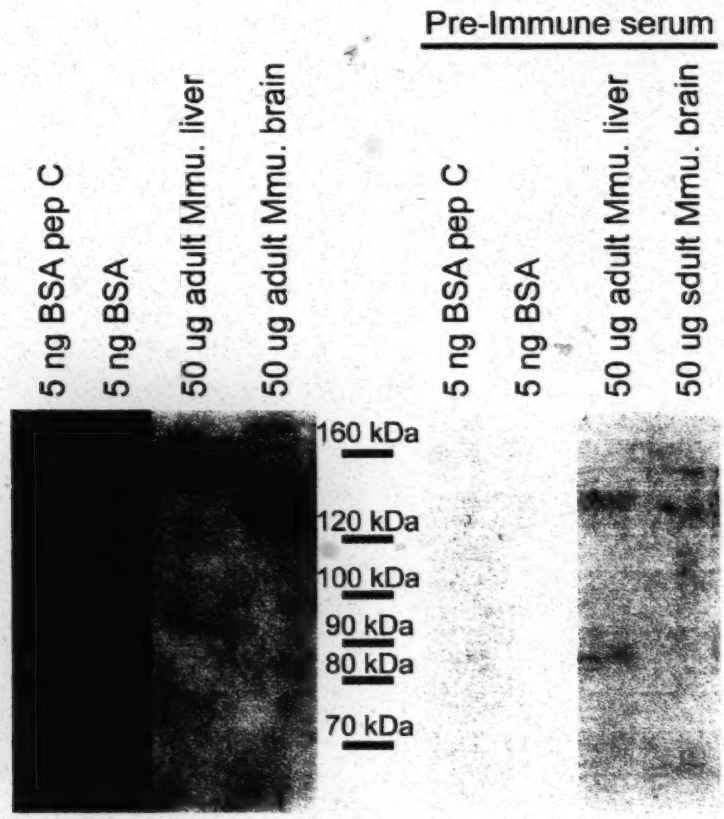

Figure 11. Western blot analysis to determining the specificity of the anti-Cecr2 pepC antibody in mouse tissues. Anti-Cecr2 pepC antibody serum from rabbit 2I6 appears to have specificity for its peptide-BSA conjugate. It also detects two different isoforms of the Cecr2 protein in adult mouse liver and brain. The signal at ~80 kDa in the Cecr2 pepC-BSA lane is the correct size. The two different signals seen in adult mouse liver at ~160 kDa and adult mouse brain at ~140 kDa are the correct sizes to be different isoforms of the Cecr2 protein. Transcripts 1-24 on Figure 7 would produce proteins approximately 160 kDa, transcripts 25-48 approximately 140 kDa and transcripts 49-72 approximately 130 kDa. The BSA negative control is blank, as is the pre-immune blot with the same samples loaded.

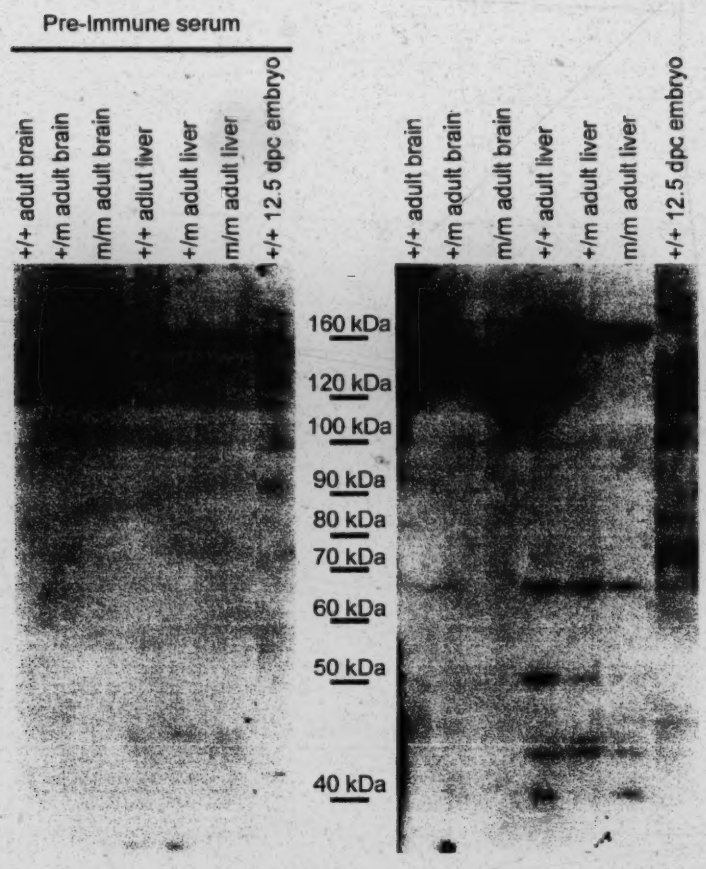

Figure 12. Transcriptional read-through occurs past the *Cecr2*^{Gt45Bic} genetrap mutation and the anti-Cecr2 pepC antibody detects the resulting protein in heterozygous and homozygous mutant mice. The two different signals seen in wild type adult mouse liver at ~160 kDa and wild type adult mouse brain at ~140 kDa are the correct sizes to be different isoforms of the Cecr2 protein. The signals are also detected in heterozygous and homozygous mutant adult mouse liver and brain lanes. The *Cecr2*^{Gt45Bic} mutant allele should halt transcription at introns 7 of the gene. However, the signals detected by the anti-Cecr2 pepC antibody, which detects an antigen C-terminal to this transcriptional stop signal, indicating read-through is occurring. The pre-immune blot is blank with the same samples loaded.

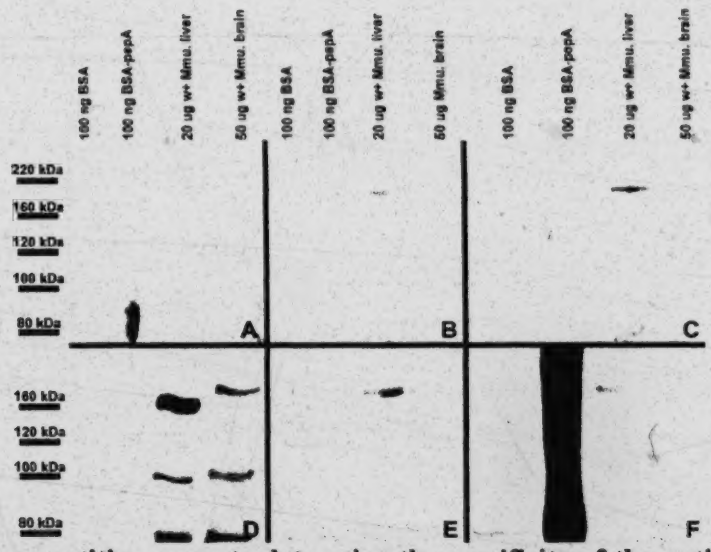

Figure 13. A competition assay to determine the specificity of the anti-Cecr2 pepA antibody using Western blot analysis. The affinity purified anti-Cecr2 pepA antibody from rabbit 2I1 appears to have specificity for the peptide it was created against conjugated to the BSA protein. The correct ~80 kDa band can be seen in the BSA conjugated to pepA lane (A). The bands detected in mouse liver (160 kDa) and brain (170 kDa) are not the same size as the bands in Figure 11, they are also seen in the pre-immune serum assay (D). These bands have since been attributed to non-specificity of the secondary antibody not the pre-immune serum. The BSA alone negative control is blank in all assays. The affinity purified 2I1 anti-Cecr2 pepA antibody was competed using 10x (B) and 50x (C) pepA-BSA. In both cases, the competed antibody was not able to bind to pepA-BSA on the membrane. This indicates that the anti-Cecr2 pepA antibody appears to have specificity for its own peptide. A mock competition using 10x (E) and 50x (F) BSA alone did not compete away the ability of the antibody to bind to Cecr2 pepA-BSA on the membrane indicating it is the peptide that is binding to the antibody and not the protein conjugate.

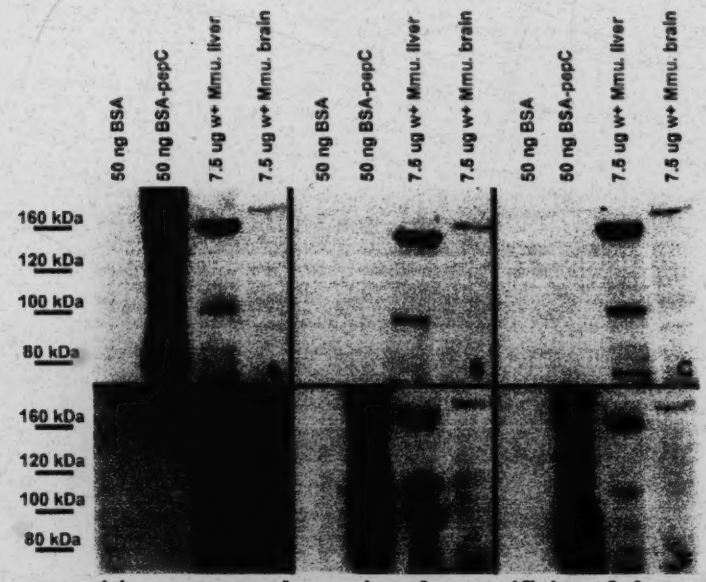

Figure 14. A competition assay to determine the specificity of the anti-Cecr2 pepC antibody using Western blot analysis. The affinity purified anti-Cecr2 pepC antibody from rabbit 2I6 appears to have specificity for the peptide it was created against conjugated to the BSA protein. The correct ~80 kDa band can be seen in the BSA conjugated to pepC lane (A). The bands detected in mouse liver (160 kDa) and brain (170 kDa) are not the same size as the bands in Figure 11, they are also seen in the pre-immune serum assay (D). The BSA alone negative control is blank in all assays. The affinity purified 2I6 anti-Cecr2 pepC antibody was competed using 10x (B) and 50x (C) pepC-BSA. In both cases the competed antibody was not able to bind to pepC-BSA on the membrane. This indicates that the anti-Cecr2 pepC antibody appears to have specificity for its own peptide. A mock competition using 10x (E) and 50x (F) BSA alone did not compete away the Cecr2 pepC-BSA band indicating it is the peptide that is binding to the antibody and not the protein conjugate. This assay was performed by Amanda Campbell, a technician in the McDermid lab.

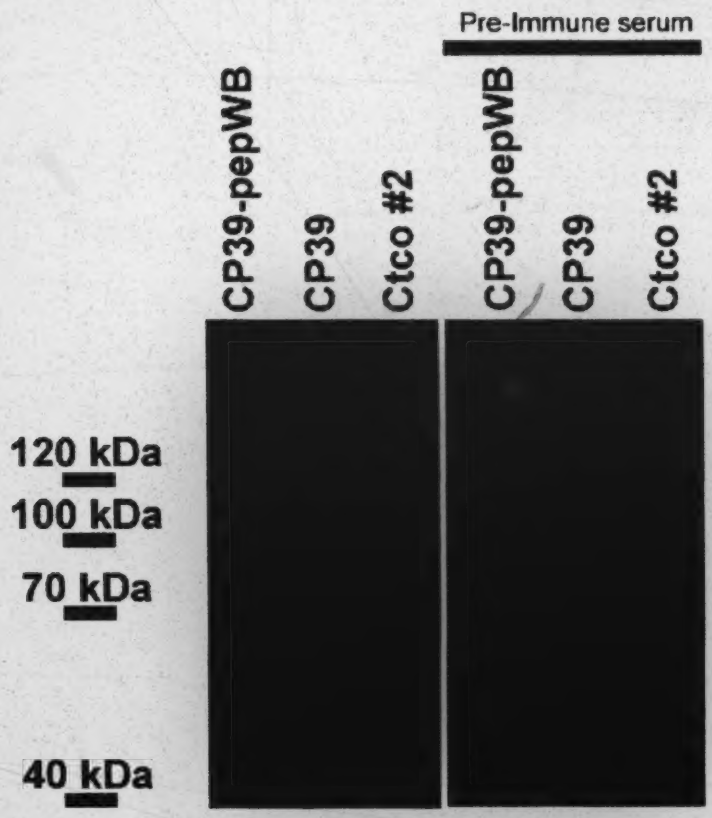

Figure 15. Preliminary testing of the anti-Cecr2 pepWB antibody using Western blot analysis. Anti-Cecr2 pepWB serum appears to have specificity for the peptide it was created against conjugated to the CP39 protein. The bands at ~40 kDa and ~110 kDa (red arrowheads) are around the correct sizes for pepWB conjugated to CP39 protein and the insect cell expressed second half of CECR2 (Ctco#2) respectively. The CP39 protein alone negative control is blank as is the pre-immune blot with all the same samples.

Chapter 4. Discussion

4.1. Mouse genetic background affects the penetrance of the NTD exencephaly in mice homozygous for the *Cecr2*^{Gt45Bic} mutation.

The exencephaly phenotype associated with the *Cecr2*^{Gt45Bic} mutation has been observed on five different mouse genetic backgrounds in this study. On each genetic background the penetrance of exencephaly was statistically different, ranging from 0% on an FVB/N genetic background to 74% on a BALB/c genetic background. On the BALB/129P2/FVB mixed genetic background, the penetrance was intermediate at 36%.

Cecr2^{Gt45Bic} is not the only NTD mouse model with variable penetrance on different genetic backgrounds. Mutants affected by genetic background include *Exencephaly* (*xn*), *Axd*, *Sp*, *ct* and *opb* (Harris and Juriloff 1997). Not only can genetic background affect the penetrance of the NTD that develops but also the phenotype associated with the mutation. For example, in *Ski* homozygous mutant mice, the phenotype and penetrance of exencephaly and other defects change as the mutation is moved from a 129P2/C57BL6 genetic background to an incipient congenic C57BL6/J genetic background (Colmenares et al. 2002). The incidence of exencephaly drops from 85% on the mixed background to only 11% after six generations of backcrossing to C57BL6/J. However, facial clefting increases from 15% on the mixed background to 78% after six generations of backcrossing to C57BL6/J. The incidence of other defects such as facial flattening, broad forehead, widely separated eyes, hexadactyly and malformed eyes and olfactory bulb increases on a C57BL6/J genetic background.

In the *opb* mutants approximately 23% of homozygous mutant embryos develop exencephaly on a mixed outbred Albino background (NMRI) (Gunther et al. 1994).

However, as the *opb* mutation was mated onto the C57BL6/J genetic background the penetrance of exencephaly decreased. *Opb* mice have excessive Shh signaling. Shh signaling causes ventralization of the neural tube by creating a region of neuroectoderm called the floor plate. If the level of Shh increases a greater area of the neuroectoderm will become floor plate (Sadler 2005). Consequently, in *opb* mutants with excessive Shh signaling an extended floor plate develops. The neural folds cannot get close enough for fusion to take place in the cranial region and the mice therefore develop exencephaly (Gunther et al. 1994; Copp et al. 2003). This penetrance difference on the two genetic backgrounds may indicate that the C57BL6/J genetic background is less sensitive to Shh signaling. Therefore, fewer mutants have an extended floor plate and, as a result, fewer mutants fail to close their cranial neural tube.

In *ct* mutants, NTDs also develop at different penetrance levels on different genetic backgrounds (van Straaten and Copp 2001). The highest penetrance, 18.5%, is on a C57BL6/J genetic background. The lowest penetrance, 2.2%, is on a DBA/2 genetic background (van Straaten and Copp 2001). Again it is likely that genetic loci differing between the C57BL6/J and DBA/2 genetic backgrounds modify neural tube closure. Therefore, mutation in the gene affecting the *ct* mutants is likely involved in the aspect of neurulation that differs between the two genetic backgrounds.

Due to observation of previous models discussed above, it is not surprising that genetic background affected the penetrance of exencephaly caused by the *Cecr2*^{Gt45Bic} mutation. However, it was surprising that none of the 45 homozygous mutant FVB/N mutant mice developed exencephaly **(Table 1)**. Changes in penetrance values indicate genetic modifiers that affect the process of neurulation exist in the different mouse

genetic backgrounds. The dramatic difference in the penetrance of exencephaly on BALB/c and FVB/N genetic backgrounds, as well as the availability of microsatellite markers that differ between the two strains, make this a unique mouse model to study potential modifier genes that affect neurulation, Cecr2 function or both.

4.2. The FVB/N mouse genetic background has one or more modifier genes that affect neural tube closure and/or Cecr2 function.

The SELH/Bc mouse strain carries a spontaneous genetic mutation that prevents neurulation closure point 2 from forming **(Figure 1)** (Macdonald et al. 1989). Consequently, 17% of SELH/Bc embryos develop exencephaly but no other defects. The other 83% of embryos successfully close their neural tube without closure 2 (Macdonald et al. 1989). This mouse model has many similarities to human anencephaly. It has been used to study neurulation in the hopes of determining genetic risks that may cause susceptibility in humans to developing anencephaly. One similarity is that both human anencephaly and exencephaly in the SELH/Bc strain are non-syndromic with multiple genetic and environmental risk factors contributing to their development (Juriloff et al. 1989; Macdonald et al. 1989; Botto et al. 1999). A second similarity is that there is some evidence that closure point 2 may not exist in human embryos (O'Rahilly and Muller 2002). The neural tube may instead make initial fusion at similar areas to closure 1 and closure 3 sites described in the mouse, zip up from these two sites, and end with the closing of the rostral and caudal neuropores (O'Rahilly and Muller 2002). A final reason is that there are a greater proportion of female embryos, 66%, that develop exencephaly in the SELH/Bc mouse line. A similar proportion of human anencephalic embryos are female (Juriloff et al. 1989; O'Rahilly and Muller 2002). Many other mutant mouse

models are lethal *in utero*, have other developmental defects, or develop a closure 2 site making the SELH/Bc strain a more ideal model to study potential molecular signals that may be important during mammalian neurulation.

The *Cecr2*^{Gt45Bic} mutant mouse shows many similarities to the SELH/Bc strain, including the non-syndromic nature of the mutation and the female predominance of exencephaly shown in this study, which will be discussed in the next section. These similarities may make *Cecr2*^{Gt45Bic} another candidate to study genes that may cause a susceptibility to developing anencephaly in humans.

It is hypothesized that there are genetic components that cause a susceptibility to developing exencephaly in both mice and humans (Macdonald et al. 1989). This hypothesis is applied to explain why some SELH/Bc mice develop exencephaly while others do not. Based on statistical modeling there is likely a threshold that certain undetermined environmental and genetic factors exacerbate. Based on statistical modeling using penetrance values from SELH/Bc mice backcrossed to normal strains, there are likely 2 or 3 genes responsible for the susceptibility of exencephaly (Juriloff et al. 1989).

In order to map genetic loci that differ between the BALB/c and FVB/N genetic backgrounds that may affect neurulation, a similar strategy to that used in studying the SELH/Bc model was used by graduate student Courtney Davidson. She began this project by crossing heterozygous *Cecr2*^{Gt45Bic} BALB/c mice to homozygous mutant *Cecr2*^{Gt45Bic} FVB/N mice and observing the penetrance of exencephaly in these mixed genetic background embryos. In this cross all embryos should be heterozygous for all modifier genes (BALB/FVB). The penetrance of exencephaly in the homozygous

mutants dropped to approximately 3% indicating that there may be a dominant modifier gene(s) involved in cranial neurulation present in the FVB/N genetic background. Due to the low penetrance of exencephaly and the need to collect 100 exencephalic embryos to make the data statistically significant, heterozygous mice of this BALB/FVB mixed genetic background were backcrossed to *Cecr2*^{Gt45Bic} heterozygous BALB/c mice. The penetrance of exencephaly in this backcross rebounded to approximately 28% again, indicating a dominant modifier gene(s). Reciprocal crosses were performed in both crosses (Courtney Davidson personal communication).

Embryos from the above backcross were collected and 100 exencephalic embryos, as well as 100 normal littermates, were sent to Lucy Osborne at the University of Toronto to be genotyped at over 100 microsatellite markers spaced approximately 20 cM apart. The exencephalic embryos should mostly have been BALB/BALB at all modifier loci as the penetrance of exencephaly for BALB/FVB is only 3%. Conversely, normal littermates may have been BALB/BALB or BALB/FVB. The goal was to find areas where the majority of exencephalic embryos were BALB/BALB and the majority of the normal littermates were BALB/FVB at the same loci. A promising region on chromosome 19 was identified and is currently being investigated for potential modifier gene(s) (Courtney Davidson personal communication).

Courtney Davidson has also been studying neurulation in normal BALB/c and FVB/N strains. She has been dissecting 8.5-9.5 dpc embryos looking for the location of closure 2 on the two different genetic backgrounds. She has found that both strains appear to make closure 2 contact at the forebrain midbrain boundary, which is considered normal **(Figure 1)**. However, preliminary data suggests that the FVB/N strain may make this contact

earlier in development based on somite number (Courtney Davidson personal communication). As closure point 2 appears to be occurring at approximately the same location in the two mouse genetic backgrounds, it is likely that the modifier genes are not affecting closure point location but some other process important in cranial neurulation. The modifier(s) may affect cranial mesenchyme proliferation, apoptosis regulation, actin microfilament contraction, neuroectoderm proliferation, neural crest emigration or other pathways involved exclusively in cranial neurulation (Copp 2005). Further investigation into the pathways disrupted by the *Cecr2*^{Gt45Bic} mutation as well as Cecr2 function during neurulation will help determine which modifier genes are altering neurulation in these two strains. The fact that closure 2 location does not differ between the two strains may make this an even better candidate to determine genes that may affect human cranial neurulation. If closure 2 is not present in humans, genes that modify the location of closure 2 may not cause a susceptibility to developing anencephaly in humans and may only function in modifying mouse neurulation.

4.3. Female embryos that are homozygous for the *Cecr2*^{Gt45Bic} mutation develop exencephaly at a higher frequency than males.

In the analysis of homozygous mutant embryos that develop exencephaly, it was noted that in the BALB/129P2/FVB and BALB/c genetic backgrounds approximately 66% of the embryos that developed exencephaly were female **(Table 5)**. Female predominance of exencephaly has been shown to occur in many mouse models of NTDs including *ct* (van Straaten and Copp 2001), *p53* (Sah et al. 1995), *Sp* (Goulding et al. 1993), *Neurofibromin* (*Nf1*) (Lakkis et al. 1999), SELH/Bc (Juriloff et al. 1989), NZW, *Circletail* (*Crc*), *xn* (Juriloff and Harris 2000; Copp et al. 2003; Copp 2005) and *Ephrin-*

A5 (*Efna5*) (Holmberg et al. 2000). In humans, anencephaly but not spina bifida has also been shown to be more prevalent in females than in males with a male/female ratio between 0.33 and 0.66 (Brook et al. 1994; Seller 1995).

Since the gonads are not developed at the time of neural tube closure, the predisposition of females to exencephaly is likely not due to hormonal differences between the sexes (Harris and Juriloff 1997). The difference must therefore be due to chromosomal differences between the sexes. Since some male embryos do develop exencephaly it is likely that chromosomal gender is not causative but is modifying the risk of developing exencephaly.

There has been much speculation that human males may be less susceptible to anencephaly because they develop more quickly than female embryos. However, in a study of *ct* mutant mice, although male embryos appear more developed and larger at the same day of development, the rate of growth and development in males and females does not differ (Brook et al. 1994). Another speculation is that some male embryos that develop exencephaly die *in utero* and are not therefore not detected. However, several mouse models render this theory unlikely as the total number of male and female embryos are similar (Brook et al. 1994; Harris and Juriloff 1997; Copp 2005).

There are three current hypotheses still under investigation to explain why females develop exencephaly more often than males. All three centre on X-inactivation in the female embryo. All cells in the female embryo must inactivate one of their X chromosomes. One hypothesis is that during cranial neural tube closure X-inactivation is not complete in all cells (Brook et al. 1994; Harris and Juriloff 1997). Therefore, those cells that have not inactivated one of their X chromosomes have an increase dosage of

some genes. This may disrupt cranial neural tube closure in some female embryos specifically. Another hypothesis is based on the fact that as X-inactivation occurs by methylation of one of the X chromosomes in each female cell; this may cause a depletion of methyl groups in female cells (Harris and Juriloff 1997). If cranial neural tube closure requires methylation there may not be enough methyl groups present in these cells to complete neural tube closure properly in some females. A third hypothesis is that there may not be enough neuroepithelial cells present in female embryos as cell cycle rates are slower in female cells due to the increase amount of DNA to be replicated (2% greater DNA in females) (Brook et al. 1994). This may not allow the cranial neural folds of some female embryos to be close enough for fusion to occur.

Due to the fact more female *Cecr2*^{Gt45Bic} mutant embryos develop exencephaly on a BALB/c genetic background and there is a penetrance difference between BALB/c and FVB/N genetic backgrounds, Courtney Davidson is also looking for potential X-linked modifier gene(s) in her linkage analysis. Any modifier genes located on the X chromosome will be studied for their potential role in cranial neurulation (Courtney Davidson personal communication).

4.4. *Cecr2* expression is widespread at the time of neural tube closure but shows more localized expression at later developmental stages.

On a BALB/129P2 mouse genetic background at 9.5 dpc, the approximate time of neural tube closure, *Cecr2* expression is widespread throughout most of the embryo **(Figure 6)**. In one homozygous mutant embryo at 9.5 dpc, an interesting striated pattern of staining is detected on the inside of the neural folds **(Figure 6 A)**. This may be differential staining of the rhombomeres but needs more investigation first to determine if

the pattern is reproducible and by sectioning the embryos. By 12.5 dpc on BALB/129P2 and BALB/c genetic backgrounds *Cecr2* is more specifically expressed in the brain, spinal column, spinal ganglia, eyes, nasal cavities and mesenchyme of the limbs **(Figure 5)**. The liver and heart do not appear to have any *Cecr2* expression between 9.5 and 13.5 dpc on BALB/129P2 (Banting et al. 2005) and BALB/c **(Figure 5 and 6)** genetic backgrounds.

As LacZ staining occurs in many tissues other than the neural tube it is likely that Cecr2 is involved in other developmental processes. To discover what other developmental processes may be affected by *Cecr2* mutation, a second mouse genetrap mutation has been used to produce a new line of *Cecr2* mutant mice. The new genetrap is located within intron 9 of *Cecr2* and the mutation is called $Cecr2^{GtXE769BG}$. Preliminary work by Jennifer Pockrant shows that the LacZ staining pattern between 9.5 and 13.5 dpc appears similar to that attributed to the $Cecr2^{Gt45Bic}$ allele (data not shown).

One process under investigation in the McDermid lab is the development of the reproductive system, as there is some preliminary evidence of fertility problems in male $Cecr2^{Gt45Bic}$ non-penetrant homozygous mutant mice. Therefore, undergraduate student Erica Kubanek is investigating a potential role for Cecr2 in the development of the reproductive system and the function of the adult reproductive system. A more thorough investigation of embryonic LacZ staining has uncovered staining in the developing reproductive system and mammary buds. Further investigation into a possible effect on reproduction in both males and females is underway beginning with histological examination of normal and mutant adult, and embryonic reproductive tissues at different developmental stages.

4.5. Three anti-Cecr2 antibodies were created and used to confirm that Cecr2 protein is expressed past the genetrap in homozygous mutant *Cecr2*^{Gt45Bic} mice.

The *Cecr2*^{Gt45Bic} mutation is not a null mutation. There is transcriptional read-through occurring past the genetrap. This was initially demonstrated by Graham Banting using PCR amplification past exon 7 of *Cecr2* in homozygous mutant mouse cDNAs (Banting 2003). This has also been demonstrated in a quantitative manner by technician Adam Tassone and myself using TaqMan quantitative real time PCR. In 15.5 dpc embryos, there is a 2 fold decrease in *Cecr2* expression in the heterozygotes and a 17-25 fold decrease in *Cecr2* expression in the *Cecr2*^{Gt45Bic} homozygous mutants compared to wild type (data not shown). Thus, Cecr2 expression is decreased in both heterozygotes and homozygous mutants but not completely absent in the homozygous mutants. This transcriptional read-through was confirmed at the protein level using anti-Cecr2 antibodies, developed in this study, recognizing epitopes past the Cecr2 genetrap insertion. Two isoforms of the Cecr2 protein were detected in adult mouse liver and brain **(Figure 12)**. The intensity of the protein bands in the wild type, heterozygous and homozygous mutant mouse tissue does not appear to differ. A more thorough investigation into which isoform(s) of the protein are present in 9.5 dpc embryos as well as mutant 9.5 dpc embryos that have failed to close their neural tube may shed light on which isoform(s) of the protein is/are important during neurulation.

4.6. There are 2 main splice variants of *Cecr2*.

As seen in the RT-PCR performed in this study **(Figure 8 and 9)**, at least two splice variants of *Cecr2* are expressed in adult brain, liver and kidney as well as 12.5 and 15.5 dpc embryo. In RT-PCR performed by Graham Banting using human RNA, at least six

different splice variants were found to be expressed in different tissues (Graham Banting personal communication). It is possible that one of the splice variants detected in mouse tissues plays a role in neurulation and the other splice variants play roles in other developmental processes. It is also possible that additional splice variants of *Cecr2* exist but have not yet been detected. A thorough spatial and temporal study of splicing in mouse has not yet been performed. It will be of interest to look at Cecr2 expression in a quantitative manner at 9.5 dpc, the approximate time of neural tube closure, to determine which splice variants of *Cecr2* are expressed as well as if any of the splice variants are not expressed in homozygous mutant embryos that have failed to close their neural tube.

However, alternative splicing in humans and mice can accomplish different goals. This was eloquently shown by Barak et al. 2004. In the Barak study, SNF2L, a *Drosophila* ISWI homologue and chromatin remodeling protein, has a different expression pattern in humans and mice. In humans, SNF2L is ubiquitously expressed, whereas in mice Snf2l is expressed only in the brain and developing gonads. However, in humans, SNF2L is only active in the brain and a few other tissues. This is because of an alternatively spliced variant of *SNF2L* called *SNF2L+13,* which is expressed in non-neural tissues. SNF2L+13 cannot remodel chromatin because the extra exon disrupts the SNF2 domain necessary for ATP dependent chromatin remodeling activity, therefore acting as a dominant negative. In mice, Snf2l is only expressed in tissues in which is has a function. This demonstrates a major difference in expression regulation in humans and mice.

Alternative splicing of *CECR2/Cecr2* may play a similar role as in the SNF2L/Snf2l example above, as it appears the *Cecr2* splice variants in humans and mice differ.

Human tissues tested express as many as six splice variants whereas only two splice variants have been detected to date in mice **(Figure 8 and 9)**. It is interesting that in mice exon 8 is commonly spliced out (exon 8 has also been shown to be spliced out in humans). At this time, no protein domain has been identified that spans exon 8. It would be interesting to determine if the removal of exon 8 produces an as yet unidentified protein domain between exons 7 and 9. If this were the case the splicing out of exon 8 could be very important to Cecr2 protein function as one of the different protein isoforms could create a dominant negative.

4.7. Is CERF involved in neurulation?

Snf2l, the CECR2 binding partner in the CERF complex, is expressed in adult mouse brain cortex and cerebellum, as well as the ovaries, uterus, testis and placenta. *Snf2l* expression has also been examined from 9.5 to 15.5 dpc embryonic stages. Northern blot and RNA *in situ* hybridization of mouse embryos indicates that *Snf2l* expression is at a low level throughout the embryo at 9.5 dpc and increases from 11.5 to 15.5 dpc, but remains non-specific (Lazzaro and Picketts 2001). *Snf2l* expression also increases in postnatal brains (Lazzaro and Picketts 2001). On the other hand, the other mammalian ISWI homologue, *Snf2h*, is more strongly expressed in the testis than *Snf2l*, shows similar expression in the ovaries and uterus compared to *Snf2l*, and has a much lower expression in the brain and placenta compared to *Snf2l*. *Snf2h* expression also decreases from 9.5 to 15.5 dpc and shows further decrease in expression in postnatal brain. RNA *in situ* hybridization did indicate that although *Snf2h* is also expressed throughout the embryo from 9.5 to 15.5 dpc, there is an elevated amount in the neocortex, cerebellum, olfactory

epithelium, lungs, kidneys and gut (Lazzaro and Picketts 2001). This elevated expression drops off after 15.5 dpc of gestation.

As *Snf2l* is not strongly expressed during neurulation and shows elevated expression in postnatal mouse brains, it is predicted to play a role in neuronal differentiation and dendritic branching. It is therefore likely that CeRF does not play a role in neurulation. In fact, as *Cecr2* and *Snf2l* are both expressed in adult brain it is more likely that CeRF has a role in neuronal differentiation (Lazzaro and Picketts 2001; Banting et al. 2005). The two genes are also expressed in the developing reproductive organs and therefore the CeRF complex may have a role in the development of the reproductive organs. This also indicates that Cecr2 likely forms complexes with other proteins expressed during neurulation such as Snf2h and thus another Cecr2 containing complex may have a role in cranial neural tube closure.

In the Banting et al. 2005 study, when the CERF complex was discovered, not only did SNF2L appear to associate with CECR2 but with SNF2H as well. This was determined by immunoprecipitation of Flag-CECR2 from HEK293 cell nuclear extracts using an anti-Flag antibody. From this immunoprecipitation, Flag-CECR2 was detected as well as SNF2L and SNF2H using silver staining and immunoblot analysis (Banting et al. 2005). The production of a complex between Snf2h and Cecr2 is being pursued in the McDermid lab as well as any other complexes that may form with Cecr2. The McDermid lab will also be investigating what gene(s) are under the control of the CeRF complex and other Cecr2 containing complexes.

ISWI containing complexes in other organisms such as yeast, *Drosophila* and *Xenopus* have been used to study which genes are regulated by different ISWI complexes. For

example, in *Xenopus* there are two nearly identical *ISWI* homologues, *xISWI1* and *xISWI2*, which form four chromatin remodeling complexes. Three of these complexes have equivalent complexes in humans: ACF, CHRAC and WICH (Dirscherl et al. 2005). The subunits of the fourth complex have not been determined to date. *Xenopus ISWI1/2* has been shown to be expressed in hypaxial muscle, neural tissue (including neural folds, brain and spinal cord), and otic vesicles of developing frogs (Dirscherl et al. 2005). A morpholino against *xISWI1/2* and an antisense RNA cause gastrulation, neurulation, and eye defects.

One or more xISWI complexes regulate the expression of *BMP4*, *Shh*, *Sox 9*, and *Pax6* (Dirscherl et al. 2005). *BMP4* expression in antisense and morpholino injected embryos increases compared to controls and *Shh*, *Sox 9* and *Pax6* expression in morpholino or antisense *xISWI* injected embryos is decreased compared to controls. Expression of the non neural gene *MyoD* is not affected (Dirscherl et al. 2005). All of this was shown using real time RT-PCR. Chromatin immunoprecipitation (ChIP) analysis was then used to demonstrate that one or more ISWI chromatin remodeling complex(es) in *Xenopus* bind *in vivo* to the *BMP4* promoter. This binding decreases *BMP4* expression during neurulation in wild type *Xenopus* embryos. The non neural gene MyoD did not have any ISWI binding at its promoter *in vivo* (Dirscherl et al. 2005).

As one of the *Xenopus* ISWI containing complexes does not have an identified binding partner, this could be the CERF complex. If *Xenopus* CERF was found to be the chromatin remodeling complex altering one or more of *BMP4*, *Shh*, *Sox9* and *Pax6* expression, it would be more plausible that CeRF has a role in mouse neurulation. However, much work would need to be done in *Xenopus* to confirm such a speculation.

4.8. Future directions

There are four major areas of investigation that should be pursued based on this study. The first is to determine if the CERF complex forms in mice and if Cecr2 forms any other complexes. The second is the characterization of the *Cecr2* mouse mutants to determine what role Cecr2 has during neurulation. The third is an investigation of the BALB/c and FVB/N genetic backgrounds to determine which neurulation specific modifier genes differ between the strains, which part of neurulation is affected by these genes and if there is a sex linked difference in neurulation. The final area of investigation concerns the other roles Cecr2 may have in development.

4.8.1. Confirm the CERF complex forms in mice and determine if Cecr2 is involved in any other complexes.

The identification and preliminary characterization of the CERF complex was performed in human cell lines (Banting et al. 2005). Therefore, before continuing with an investigation of CeRF in mouse, the formation of a complex between mouse Snf2l and Cecr2 should be confirmed in mouse cell lines. The anti-Cecr2 antibody(ies) developed in this study could be used to confirm the formation of the CeRF complex in mouse. This could be done by expressing mouse Cecr2 in a mouse cell line and performing protein pull downs from these cells. The proteins could then be separated on a polyacrylamide gel and the bands cut out and sent for mass spectroscopy to confirm their identity. This technique should first be used to confirm the specificity of the current anti-Cecr2 antibodies and then to determine which proteins are associated with Cecr2. If the antibody developed in this study cannot be used, a flag tag Cecr2 could be used instead

and an anti-flag antibody used to immunoprecipitate any complexes that may form. I expect that not only will Snf2l be identified as a Cecr2 binding partner but also Snf2h.

It would also be beneficial to begin an investigation into which gene targets the CeRF complex may associate with. As CeRF is a chromatin remodeling complex, determining which genes CeRF targets may help identify its role in development. This can be done by using genes identified as ISWI targets in other organisms such as *Xenopus*. Once potential gene targets are identified, the expression level of these genes can be investigated using quantitative real time RT-PCR. This should be done in normal and $Cecr2^{Gt45Bic}$ mutant mice to determine if the target gene(s) expression is misregulated when one of the complex proteins is knocked down. *In vivo* association at the promoter of potential CeRF gene targets can be identified using Chromatin immunoprecipitation. Both anti-Cecr2 antibodies as well as anti-Snf2l antibodies should be used in this analysis. Genes whose promoter regions show association with both Snf2l and Cecr2 should be considered targets for the CeRF complex. If the promoter only shows an association with Cecr2, it is likely that another complex that forms with Cecr2 controls the expression of that particular gene, perhaps one involving Snf2h. It is likely that non-overlapping gene targets will be identified for Cecr2 and Snf2l because both genes may have roles in other protein complexes. In humans, SNF2L has already been shown to be a component of the hNURF complex and responsible for the transcriptional regulation of *engrailed-1* and *engrailed-2* (Barak et al. 2003). It would be illuminating to determine which genes are regulated by CeRF and what developmental role the CeRF complex has.

4.8.2. Characterization of the *Cecr2* mouse mutants to determine the role Cecr2 plays during neurulation.

Microarray analysis on the *Cecr2*^{Gt45Bic} mutant mouse model could be used to begin determining a role for Cecr2 in neurulation. RNA from embryos before, during and after neural tube closure from both wild type and mutant mice could be analyzed to determine which transcripts are up or down regulated in the mutant mice. Ultimately, microarray analysis could identify multiple targets of Cecr2 and potentially CeRF or other Cecr2 containing complexes. The specific process within neurulation affected, as well as other potential developmental roles for Cecr2, could be elucidated from determining the function of these target genes.

In order to pinpoint a more specific role for Cecr2 during neurulation, the *Cecr2*^{Gt45Bic} mouse line can be used to determine what process(es) are disrupted when *Cecr2* expression is knocked down. In other mouse mutants that develop exencephaly, many known cellular processes such as cell proliferation, apoptosis, actin microfilament contraction and cell migration are disrupted (Copp 2005). For instance, actin microfilament contraction is disrupted in *vinculin*, *MARCKS*, *Mena*, *profiling 1* and *shrm* mouse mutants. In *shrm* mutant mice, the cytoskeletal polarity in the neuroepithelium is disrupted and the neural tube does not become properly shaped. Shrm binds to F-actin and directs its subcellular localization (Hildebrand and Soriano 1999). Therefore, in *shrm* null mice, F-actin is not properly localized to the apical surface of cells at the cranial neural folds. This inhibits the neuroepithelial cells from taking on the proper shape. This shape is likely important for the formation of the DLHPs to form and, therefore, the DLHPs do not form properly in *shrm* null mice. The mice consequently

develop exencephaly and occasionally spina bifida (Haigo et al. 2003). Therefore, one mechanism to study in the *Cecr2* mouse mutants is the localization and apical constriction of actin microfilaments at the DLHPs just before neural tube closure. If this process is disrupted, Cecr2 likely has a role in cytoskeletal polarity. Another pathway often affected in mouse mutants that develop exencephaly is neuroepithelial proliferation (Copp 2005). Examples of mouse mutants with defects in neuroepithelial proliferation include *RBP-Jκ*, *Hes1* and *Numb* (Copp 2005). Cell proliferation in the cranial region at the approximate time of neurulation can be investigated using BrdU staining in wild type and $Cecr2^{Gt45Bic}$ mutant littermates. If *Cecr2* mutant mice show a decrease in the proliferation of cranial mesenchyme and neuroepithelium, then Cecr2 could be inferred to have a role in that area of cranial development necessary for proper neurulation. Similar experiments should be done using TUNEL staining to determine if appropriate levels of apoptosis in the appropriate cell types are occurring in $Cecr2^{Gt45Bic}$ mutant animals at the time of neural closure. Apoptosis is misregulated in *Apaf1*, *Caspase 9* and *Bcl10* mutant mice, which all develop exencephaly (Copp 2005). The emigration of neural crest cells from the cranial neural folds should also be investigated as this process is disrupted in *Sp*, *Connexin43*, *Cited2* and *Twist* mutant mice, which all develop exencephaly (Copp 2005).

Dietary supplements such as folic acid and inositol have been shown to affect neurulation and have preventative roles in some NTD causing mouse mutants (Copp et al. 2003). Folic acid has been identified as preventing as many as 70% of human NTDs and likewise many but not all mouse mutants tested are folate sensitive (Botto et al. 1999; Copp et al. 2003). Folate sensitive mouse mutants include *Sp*, *Cart1*, *Crooked tail* and

Cited2. However, *ct*, *Axd* and *EphA7* mutants are folate resistant (Copp et al. 2003). In the folate resistant *ct* mice, inositol prevented spinal NTDs (van Straaten and Copp 2001). A folate study was performed in the *Cecr2*^{Gt45Bic} mutant mice on the BALB/129P2 genetic background (Banting 2003). No rescue effect was associated with the supplementation of pregnant dams with folate compared to saline injected controls (Banting 2003). It would be interesting to repeat this study on the BALB/c genetic background to determine if genetic background affects the response to folate in the *Cecr2* mutant mice. It would also be interesting to treat the mice with inositol and look for a rescue effect on the exencephaly phenotype. Determining if these or other dietary supplements could decrease or exacerbate the penetrance of exencephaly in *Cecr2* mutant mice would be useful in directing the study of Cecr2 towards a developmental pathway.

Finally, RNA *in situ* hybridization with patterning and cell fate markers should be performed to further characterize the molecular pathways that are disrupted in *Cecr2*^{Gt45Bic} mutant mice. For example, *Shh* is a floor plate marker that has been used to investigate patterning in zebrafish, *Xenopus* and mice (Gunther et al. 1994; Lowery and Sive 2004; Dirscherl et al. 2005; Wilson and Maden 2005). Roof plate markers including *Wnt3a*, *Wnt1*, *BMP6*, and *MSX1* can also be used to determine if the roof plate of the neural tube is forming correctly in the *Cecr2*^{Gt45Bic} mutant mice (Gunther et al. 1994). Using these neurulation markers on *Cecr2*^{Gt45Bic} mutant mice and comparing the expression to normal littermates may allow more subtle defects in neural tube formation to be detected. Again, this may help focus the study of Cecr2 to a particular part of neurulation.

4.8.3. Investigate the BALB/c and FVB/N genetic backgrounds to determine what neurulation specific modifier genes differ between the strains, what part of neurulation is affected by these genes and if there is a sex linked difference in neurulation.

As previously mentioned, graduate student Courtney Davidson has been analyzing the BALB/c and FVB/N genetic backgrounds for the presence of neurulation modifying genes. She has located a region on chromosome 19 that appears to contain one or more modifier genes. She has been investigating closure 2 in the two genetic backgrounds as well and it appears that the closure 2 location does not differ in the strains, but the FVB/N strain appears to initiate closure 2 earlier in gestation based on somite number. It is therefore likely that modifier genes affect neurulation processes other than the closure 2 contact site.

4.8.4. The role of Cecr2 in other developmental pathways.

As Cecr2 appears to be expressed in many tissues over the course of embryonic development, it would be of interest to determine what, if any, role Cecr2 has in the development of the reproduction system, eyes, limbs, nasal epithelium and mammary glands. This project has been initiated for reproductive organs using histological sections of LacZ stained normal and mutant testis and ovary, as well as at different embryonic stages to investigate the gonads (Erica Kubanek personnel communication).

4.9. Significance of this work

In the current study, I have developed three anti-Cecr2 antibodies that can be used to further the investigation of the developmental role of Cecr2 in mice. I have also demonstrated that mouse genetic background affects the penetrance of the cranial neural

tube defect exencephaly. An interesting observation was that the FVB/N genetic background appears to be resistant to exencephaly development caused by a mutation in *Cecr2*. As well, this model shows some resemblance to the human situation. For example, 66% of the mutant embryos that develop exencephaly are female in both humans and in the $Cecr2^{Gt45Bic}$ mutant mice. This study has lead to a spin off project ongoing in the McDermid lab by Courtney Davidson. She is using the penetrance difference between the BALB/c and FVB/N genetic backgrounds to determine potential neurulation modifying genes in FVB/N that may lower the susceptibility of developing a cranial NTD. She is also investigating neurulation in the two genetic backgrounds to determine how they differ and therefore what role Cecr2 has in neurulation.

I have also begun a temporal and spacial investigation of *Cecr2* expression using RT-PCR and X-gal staining. This evidence suggests *Cecr2* is expressed in several tissues other that the developing brain and neural tube. I have also detected two splice variants of *Cecr2* that are expressed in all tissues and embryonic stages tested. Using this information, an investigation into other Cecr2 developmental roles appears to be a good avenue to pursue. There is already promising evidence that Cecr2 may be involved in the development of the reproductive system. It will also be interesting to determine what role the different splice variants of *Cecr2* have in mouse. Perhaps one of the splice variants codes for a protein that has an important functional domain disrupted and therefore is not biologically active. Another possibility is that the splice variants have different *in vivo* roles. The anti-Cecr2 antibodies developed in this study indicate that there are also at least two protein isoforms of Cecr2. No matter what role Cecr2 has in

neurulation and development, it will be interesting to investigate this gene and its protein function further in an attempt to understand mouse and human development.

Chapter 5. Bibliography

Aalfs, J.D. and R.E. Kingston. 2000. What does 'chromatin remodeling' mean? *Trends Biochem Sci* **25**: 548-55.

Aalfs, J.D., G.J. Narlikar, and R.E. Kingston. 2001. Functional differences between the human ATP-dependent nucleosome remodeling proteins BRG1 and SNF2H. *J Biol Chem* **276**: 34270-8.

Aravind, L. and D. Landsman. 1998. AT-hook motifs identified in a wide variety of DNA-binding proteins. *Nucleic Acids Res* **26**: 4413-21.

Banting, G.S. 2003. Characterization of the cat eye syndrome candidate gene CECR2. In *Biological Sciences*. University of Alberta, Edmonton, Alberta, Canada.

Banting, G.S., O. Barak, T.M. Ames, A.C. Burnham, M.D. Kardel, N.S. Cooch, C.E. Davidson, R. Godbout, H.E. McDermid, and R. Shiekhattar. 2005. CECR2, a protein involved in neurulation, forms a novel chromatin remodeling complex with SNF2L. *Hum Mol Genet* **14**: 513-24.

Barak, O., M.A. Lazzaro, N.S. Cooch, D.J. Picketts, and R. Shiekhattar. 2004. A tissue-specific, naturally occurring human SNF2L variant inactivates chromatin remodeling. *J Biol Chem* **279**: 45130-8.

Barak, O., M.A. Lazzaro, W.S. Lane, D.W. Speicher, D.J. Picketts, and R. Shiekhattar. 2003. Isolation of human NURF: a regulator of Engrailed gene expression. *Embo J* **22**: 6089-100.

Berube, N.G., M. Jagla, C. Smeenk, Y. De Repentigny, R. Kothary, and D.J. Picketts. 2002. Neurodevelopmental defects resulting from ATRX overexpression in transgenic mice. *Hum Mol Genet* **11**: 253-61.

Botto, L.D., C.A. Moore, M.J. Khoury, and J.D. Erickson. 1999. Neural-tube defects. *N Engl J Med* **341**: 1509-19.

Boyles, A.L., P. Hammock, and M.C. Speer. 2005. Candidate gene analysis in human neural tube defects. *Am J Med Genet C Semin Med Genet* **135**: 9-23.

Brook, F.A., J.P. Estibeiro, and A.J. Copp. 1994. Female predisposition to cranial neural tube defects is not because of a difference between the sexes in the rate of embryonic growth or development during neurulation. *J Med Genet* **31**: 383-7.

Colmenares, C., H.A. Heilstedt, L.G. Shaffer, S. Schwartz, M. Berk, J.C. Murray, and E. Stavnezer. 2002. Loss of the SKI proto-oncogene in individuals affected with 1p36 deletion syndrome is predicted by strain-dependent defects in Ski-/- mice. *Nat Genet* **30**: 106-9.

Copp, A.J. 2005. Neurulation in the cranial region--normal and abnormal. *J Anat* **207**: 623-35.

Copp, A.J., N.D. Greene, and J.N. Murdoch. 2003. The genetic basis of mammalian neurulation. *Nat Rev Genet* **4**: 784-93.

Dhalluin, C., J.E. Carlson, L. Zeng, C. He, A.K. Aggarwal, and M.M. Zhou. 1999. Structure and ligand of a histone acetyltransferase bromodomain. *Nature* **399**: 491-6.

Dirscherl, S.S., J.J. Henry, and J.E. Krebs. 2005. Neural and eye-specific defects associated with loss of the Imitation Switch (ISWI) chromatin remodeler in Xenopus laevis. *Mech Dev* **122**: 1157-70.

Doerks, T., R. Copley, and P. Bork. 2001. DDT -- a novel domain in different transcription and chromosome remodeling factors. *Trends Biochem Sci* **26**: 145-6.

Eberharter, A. and P.B. Becker. 2004. ATP-dependent nucleosome remodelling: factors and functions. *J Cell Sci* **117**: 3707-11.

Fazzio, T.G., M.E. Gelbart, and T. Tsukiyama. 2005. Two distinct mechanisms of chromatin interaction by the Isw2 chromatin remodeling complex in vivo. *Mol Cell Biol* **25**: 9165-74.

Fazzio, T.G. and T. Tsukiyama. 2003. Chromatin remodeling in vivo: evidence for a nucleosome sliding mechanism. *Mol Cell* **12**: 1333-40.

Fleming, A. and A.J. Copp. 2000. A genetic risk factor for mouse neural tube defects: defining the embryonic basis. *Hum Mol Genet* **9**: 575-81.

Footz, T.K., P. Brinkman-Mills, G.S. Banting, S.A. Maier, M.A. Riazi, L. Bridgland, S. Hu, B. Birren, S. Minoshima, N. Shimizu, H. Pan, T. Nguyen, F. Fang, Y. Fu, L. Ray, H. Wu, S. Shaull, S. Phan, Z. Yao, F. Chen, A. Huan, P. Hu, Q. Wang, P. Loh, S. Qi, B.A. Roe, and H.E. McDermid. 2001. Analysis of the cat eye syndrome critical region in humans and the region of conserved synteny in mice: a search for candidate genes at or near the human chromosome 22 pericentromere. *Genome Res* **11**: 1053-70.

Fyodorov, D.V. and J.T. Kadonaga. 2002. Binding of Acf1 to DNA involves a WAC motif and is important for ACF-mediated chromatin assembly. *Mol Cell Biol* **22**: 6344-53.

Golden, J.A. and G.F. Chernoff. 1993. Intermittent pattern of neural tube closure in two strains of mice. *Teratology* **47**: 73-80.

Goulding, M., S. Sterrer, J. Fleming, R. Balling, J. Nadeau, K.J. Moore, S.D. Brown, K.P. Steel, and P. Gruss. 1993. Analysis of the Pax-3 gene in the mouse mutant splotch. *Genomics* **17**: 355-63.

Greene, N.D. and A.J. Copp. 2005. Mouse models of neural tube defects: investigating preventive mechanisms. *Am J Med Genet C Semin Med Genet* **135**: 31-41.

Grune, T., J. Brzeski, A. Eberharter, C.R. Clapier, D.F. Corona, P.B. Becker, and C.W. Muller. 2003. Crystal structure and functional analysis of a nucleosome recognition module of the remodeling factor ISWI. *Mol Cell* **12**: 449-60.

Gunther, T., M. Struwe, A. Aguzzi, and K. Schughart. 1994. Open brain, a new mouse mutant with severe neural tube defects, shows altered gene expression patterns in the developing spinal cord. *Development* **120**: 3119-30.

Haigo, S.L., J.D. Hildebrand, R.M. Harland, and J.B. Wallingford. 2003. Shroom induces apical constriction and is required for hingepoint formation during neural tube closure. *Curr Biol* **13**: 2125-37.

Harris, M.J. and D.M. Juriloff. 1997. Genetic landmarks for defects in mouse neural tube closure. *Teratology* **56**: 177-87.

Harris, MJ. and D.M. Juriloff. 1999. Mini-review: toward understanding mechanisms of genetic neural tube defects in mice. *Teratology* **60**: 292-305.

Hendrich, B. and W. Bickmore. 2001. Human diseases with underlying defects in chromatin structure and modification. *Hum Mol Genet* **10**: 2233-42.

Hildebrand, J.D. and P. Soriano. 1999. Shroom, a PDZ domain-containing actin-binding protein, is required for neural tube morphogenesis in mice. *Cell* **99**: 485-97.

Holmberg, J., D.L. Clarke, and J. Frisen. 2000. Regulation of repulsion versus adhesion by different splice forms of an Eph receptor. *Nature* **408**: 203-6.

Johnson, C.N., N.L. Adkins, and P. Georgel. 2005. Chromatin remodeling complexes: ATP-dependent machines in action. *Biochem Cell Biol* **83**: 405-17.

Jones, M.H., N. Hamana, J. Nezu, and M. Shimane. 2000a. A novel family of bromodomain genes. *Genomics* **63**: 40-5.

Jones, M.H., N. Hamana, and M. Shimane. 2000b. Identification and characterization of BPTF, a novel bromodomain transcription factor. *Genomics* **63**: 35-9.

Juriloff, D.M. and M.J. Harris. 2000. Mouse models for neural tube closure defects. *Hum Mol Genet* **9**: 993-1000.

Juriloff, D.M., K.B. Macdonald, and M.J. Harris. 1989. Genetic analysis of the cause of exencephaly in the SELH/Bc mouse stock. *Teratology* **40**: 395-405.

Kibar, Z., K.J. Vogan, N. Groulx, M.J. Justice, D.A. Underhill, and P. Gros. 2001. Ltap, a mammalian homolog of Drosophila Strabismus/Van Gogh, is altered in the mouse neural tube mutant Loop-tail. *Nat Genet* **28**: 251-5.

Lakkis, M.M., J.A. Golden, K.S. O'Shea, and J.A. Epstein. 1999. Neurofibromin deficiency in mice causes exencephaly and is a modifier for Splotch neural tube defects. *Dev Biol* **212**: 80-92.

Lazzaro, M.A. and D.J. Picketts. 2001. Cloning and characterization of the murine Imitation Switch (ISWI) genes: differential expression patterns suggest distinct developmental roles for Snf2h and Snf2l. *J Neurochem* **77**: 1145-56.

Lowery, L.A. and H. Sive. 2004. Strategies of vertebrate neurulation and a re-evaluation of teleost neural tube formation. *Mech Dev* **121**: 1189-97.

Macdonald, K.B., D.M. Juriloff, and M.J. Harris. 1989. Developmental study of neural tube closure in a mouse stock with a high incidence of exencephaly. *Teratology* **39**: 195-213.

Maier, S.A. 2005. Use of model organisms and phylogenetic analysis to characterize the role of *CECR1* in cat eye syndrome. In *Department of Biological Sciences*, pp. 198. University of Alberta, Edmonton.

Mimotopes Mitokor company manual. May 10, 2001. Antipeptide antibodies. p. 16.

Murdoch, J.N., D.J. Henderson, K. Doudney, C. Gaston-Massuet, H.M. Phillips, C. Paternotte, R. Arkell, P. Stanier, and A.J. Copp. 2003. Disruption of scribble (Scrb1) causes severe neural tube defects in the circletail mouse. *Hum Mol Genet* **12**: 87-98.

O'Rahilly, R. and F. Muller. 2002. The two sites of fusion of the neural folds and the two neuropores in the human embryo. *Teratology* **65**: 162-70.

Reeves, R. and M.S. Nissen. 1990. The A.T-DNA-binding domain of mammalian high mobility group I chromosomal proteins. A novel peptide motif for recognizing DNA structure. *J Biol Chem* **265**: 8573-82.

Sadler, T.W. 2005. Embryology of neural tube development. *Am J Med Genet C Semin Med Genet* **135**: 2-8.

Sah, V.P., L.D. Attardi, G.J. Mulligan, B.O. Williams, R.T. Bronson, and T. Jacks. 1995. A subset of p53-deficient embryos exhibit exencephaly. *Nat Genet* **10**: 175-80.

Sakai, Y., C. Meno, H. Fujii, J. Nishino, H. Shiratori, Y. Saijoh, J. Rossant, and H. Hamada. 2001. The retinoic acid-inactivating enzyme CYP26 is essential for establishing an uneven distribution of retinoic acid along the anterio-posterior axis within the mouse embryo. *Genes Dev* **15**: 213-25.

Seller, M.J. 1995. Sex, neural tube defects, and multisite closure of the human neural tube. *Am J Med Genet* **58**: 332-6.

Tate, P., M. Lee, S. Tweedie, W.C. Skarnes, and W.A. Bickmore. 1998. Capturing novel mouse genes encoding chromosomal and other nuclear proteins. *J Cell Sci* **111**: 2575-85.

van Straaten, H.W. and A.J. Copp. 2001. Curly tail: a 50-year history of the mouse spina bifida model. *Anat Embryol (Berl)* **203**: 225-37.

Vogelweid, C.M., D.W. Vogt, C.L. Besch-Williford, and S.E. Walker. 1993. New Zealand white mice: an experimental model of exencephaly. *Lab Anim Sci* **43**: 58-60.

Wilson, L. and M. Maden. 2005. The mechanisms of dorsoventral patterning in the vertebrate neural tube. *Dev Biol* **282**: 1-13.

http://www.jax.org/imr/controls.html